bioRxiv preprint doi: https://doi.org/10.1101/847988; this version posted November 20, 2019. The copyright holder for this preprint (which was not certified by peer review) is the author/funder. All rights reserved. No reuse allowed without permission.

Peripheral Nerve Repair Using Tissue Engineered "Living Scaffolds" Comprised of Stretch-Grown Aligned Axonal Tracts Promotes Survival of Spinal Cord Motor Neurons

Joseph C. Maggiore[1,3*], Justin C. Burrell[1,2,3*], Kevin D. Browne[2,3], Kritika S. Katiyar[2,3,4], Franco A. Laimo[2,3], Zarina Ali[2], Hilton M. Kaplan[5], Joseph M. Rosen[6], D. Kacy Cullen[1,2,3]

[1]Department of Bioengineering and [2]Department of Neurosurgery, University of Pennsylvania, Philadelphia, PA

[3]Center for Neurotrauma, Neurodegeneration & Restoration, CMC VA Medical Center, Philadelphia, PA

[4]School of Biomedical Engineering, Science and Health Systems, Drexel University, Philadelphia, PA

[5]New Jersey Center for Biomaterials, Rutgers University, New Brunswick, NJ, United States of America

[6]Dartmouth-Hitchcock Medical Center, Division of Plastic Surgery, Dartmouth College, Lebanon, NH, United States of America

*J.C.M. and J.C.B. should be considered joint first author

Corresponding author:

D. Kacy Cullen, Ph.D.
105E Hayden Hall/3320 Smith Walk
Dept. of Neurosurgery
University of Pennsylvania
Philadelphia, PA 19104
Ph: 215-746-8176
Fx: 215-573-3808
Email: dkacy@pennmedicine.med.upenn.edu

Key Words: peripheral nerve injury, spinal cord motor neuron, cell death, surgical repair, neuronal survival, retrograde tracer, tissue engineered nerve

bioRxiv preprint doi: https://doi.org/10.1101/847988; this version posted November 20, 2019. The copyright holder for this preprint (which was not certified by peer review) is the author/funder. All rights reserved. No reuse allowed without permission.

Abstract:

Peripheral nerve injury (PNI) impacts millions annually, often leaving debilitated patients with minimal repair options to improve functional recovery. Our group has previously developed tissue engineered nerve grafts (TENGs) featuring long, aligned axonal tracts from dorsal root ganglia (DRG) neurons that are fabricated in custom bioreactors using the process of axon "stretch-growth". We have shown that TENGs effectively serve as "living scaffolds" to promote regeneration across segmental nerve defects by exploiting the newfound mechanism of axon-facilitated axon regeneration, or "AFAR", by simultaneously providing haptic and neurotrophic support. To extend this work, the current study investigated the efficacy of living versus non-living regenerative scaffolds in preserving host sensory and motor neuron cell health, using retrograde dye transport as a proxy, following bridging of segmental nerve defects. Rats were assigned across five groups: naïve or repair using autograft, nerve guidance tube (NGT) with collagen, NGT + non-aligned DRG populations in collagen, or TENGs. We found that TENG repairs yielded equivalent regenerative capacity as autograft repairs based on preserved health of host spinal cord motor neurons and acute axonal regeneration, whereas NGT repairs or DRG neurons within an NGT exhibited reduced motor neuron preservation and diminished regenerative capacity. These acute regenerative benefits ultimately resulted in enhanced levels of functional recovery in animals receiving TENGs, at levels matching those attained by autografts. Our findings indicate that when used to bridge segmental nerve defects, TENGs preserve host spinal cord motor neuron health and regenerative capacity without sacrificing an otherwise uninjured nerve (as in the case of the autograft), and therefore represent a promising alternative strategy for neurosurgical repair following PNI.

bioRxiv preprint doi: https://doi.org/10.1101/847988; this version posted November 20, 2019. The copyright holder for this preprint (which was not certified by peer review) is the author/funder. All rights reserved. No reuse allowed without permission.

HIGHLIGHTS

1) TENGs preserve host spinal cord motor neuron health and regenerative capacity acutely following repair of segmental nerve defects, matching that of the clinical gold-standard autograft and exceeding commercially-available nerve guidance tubes.
2) TENGs facilitated regeneration across segmental nerve defects, yielding similar degree of chronically surviving host spinal motor neurons and functional recovery as compared to autografts.
3) Early surgical intervention for segmental nerve defect with living scaffolds, such as TENGs and autografts, preserves the host regenerative capacity, and likely increases the ceiling for total regeneration and functional recovery at chronic time points compared to (acellular) commercially-available nerve guidance tubes.
4) TENGs preserve host neuronal health and regenerative capacity without sacrificing an otherwise uninjured nerve, and therefore represent a promising alternative strategy to autografts or nerve guidance tube repairs.

bioRxiv preprint doi: https://doi.org/10.1101/847988; this version posted November 20, 2019. The copyright holder for this preprint (which was not certified by peer review) is the author/funder. All rights reserved. No reuse allowed without permission.

Introduction

It is estimated that nearly 20 million Americans suffer from traumatic peripheral nerve injury (PNI) and only 50% of patients achieve normal functional recovery following surgery.[1] Following PNI, the distal nerve segment undergoes Wallerian degeneration – a process of rapid axonal loss and myelin sheath degradation. During this process, contrary to degeneration, Schwann cells proliferate[2,3] – forming highly aligned columns, called Bands of Büngner. These facilitate regeneration[4] and maintain neuronal cell health proximally by providing a pro-regenerative environment that counteracts the cell death process induced from PNI trauma.[5,6] However, the pro-regenerative environment cannot be sustained in cases requiring long regenerative distances to the distal muscle and/or organ end-targets.[7] Moreover, prolonged denervation results in permanent muscle atrophy,[8], diminished proximal neuronal health[9], retrograde dieback of axotomized neurons,[10] and ultimately an overall lowering of regenerative capacity for functional recovery.[11-13] For this reason, a PNI repair strategy that provides a pro-regenerative environment – including maintenance of proximal neuronal cell health – is necessary to establish a more comprehensive and effective clinical repair strategy.

In particular, one important cellular process involved with maintaining neuronal cell health is retrograde transport.[14,15] Studies have shown that loss of retrograde transport in proximal neuron cell bodies reduces neuronal health during regeneration.[16,17] Following untreated PNI, retrograde transport of neurotrophic factors is inhibited in the proximal stump, concurrent with an initiation of a retrograde dieback process.[15] Over time, sustained diminished retrograde transport leads to poor neuronal cell health,[18] and regenerative capacity of proximal neurons in the spinal cord.[19,20] Thus, retrograde transport is a valuable surrogate marker for neuronal cell health and ultimately regenerative capacity. Recent studies have demonstrated that neurotrophic signals such as glial cell-line derived neurotrophic factor (GDNF), brain derived neurotrophic factor (BDNF) and nerve growth factor (NGF) secreted in the distal environment revitalize retrograde transport,[17] improve cell health,[21,22] and sustain regeneration.[23-26] Recently, biological nerve grafts have been developed containing exogenous growth factors to simulate a pro-regenerative environment. However, a bolus of exogenous growth factors is unlikely able to provide a sustainable pro-regenerative environment required for functional recovery.[27,28] Despite the recent advancements in neural engineering, autograft nerve repairs still remain the current gold standard surgical treatment due to the superior functional recovery compared to commercially available products, such as a nerve guidance tube (NGT) or acellular nerve allograft. As an endogenously-available living scaffold, autografts provide regenerating host axons with a structural support, necessary for anisotropic growth, as well as a rich supply of growth factors secreted by the

bioRxiv preprint doi: https://doi.org/10.1101/847988; this version posted November 20, 2019. The copyright holder for this preprint (which was not certified by peer review) is the author/funder. All rights reserved. No reuse allowed without permission.

Schwann cells.[29] However, autografts pose a challenging repair solution for instances of large gap repair and donor site comorbidity.

In order to compensate for the drawbacks of current PNI repair strategies, our group has previously developed tissue engineered nerve grafts (TENGs) – generated utilizing stretch grown axons encapsulated in an extracellular matrix (ECM) that simultaneously provide structural support necessary for anisotropic growth and neurotrophic support through regulated growth factor release.[30] These advantages likely play a significant role in the accelerated host nerve regeneration and enhanced functional recovery demonstrated in previously studies using TENGs.[31] While most PNI repair strategies have been well studied as they relate to regenerative and functional outcome measures (e.g., density of regenerating axons and extent of muscular recovery), there is limited information regarding the ability of various graft repair strategies to sustain proximal neuronal cell health and thereby maintain regenerative capacity. We hypothesize living scaffolds, such as autografts and TENGs, will preserve proximal neuron health and overall capacity for regeneration by providing regenerating axons with haptic and chemotaxic cues, and/or trophic support. Thus, we investigated the effect of various living (TENGS, dissociated neurons randomly distributed across ECM, and autografts) and non-living (ECM-laden nerve guidance tubes) scaffolds in maintaining the cell health of host spinal cord motor neurons and dorsal root ganglia neurons as a surrogate marker for regenerative capacity of motor and sensory axons, respectively. Within living scaffolds, this study also evaluated the effect of axonal organization, as highly organized TENGs with their architecture of defined neuronal populations spanned by long-projecting, aligned axonal tracts was compared to constructs comprised of disorganized, dissociated neurons growing randomly throughout the ECM.

Methods

All procedures were approved by the Michael J. Crescenz Veterans Affairs Medical Center Institutional Animal Care and Use Committee and adhered to the guidelines set forth in the NIH Public Health Service Policy on Humane Care and Use of Laboratory Animals (2015). All supplies were from Invitrogen (Carlsbad, CA), BD Biosciences (San Jose, CA), or Sigma-Aldrich (St. Louis, MO) unless otherwise noted.

Dorsal Root Ganglion Neuron Isolation

Dorsal root ganglia (DRG) were isolated from embryonic day 16 Sprague-Dawley rats (Charles River, Wilmington, MA). Briefly, timed-pregnant rats were euthanized, and pups were extracted through Caesarian section. Each fetus was removed from the amniotic sac and put in

bioRxiv preprint doi: https://doi.org/10.1101/847988; this version posted November 20, 2019. The copyright holder for this preprint (which was not certified by peer review) is the author/funder. All rights reserved. No reuse allowed without permission.

cold Leibovitz-15. Embryonic DRG explants were isolated from spinal cords and either plated directly into media or dissociated. For dissociation, explants were suspended in pre-warmed trypsin (0.25%) + EDTA (1 mm) at 37°C for 45 min. Followed by the addition of neurobasal medium + 5% FBS, the tissue was vortexed for at least 30 seconds and then centrifuged at 1000 rpm for 3 minutes. The supernatant was aspirated, and the cells were resuspended at $5x10^6$ cells/mL in media. Media for both dissociated cells and explants consisted of neurobasal medium + 2% B-27 + 400-500 µm L-glutamine + 1% fetal bovine serum (Atlanta Biologicals) + 2.0-2.5 mg/mL glucose + 10-20 ng/mL 2.5S nerve growth factor, and a mitotic inhibitor formulation of 10 mM 5-fluoro-2'-deoxyuridine (5FdU) and 10 mm uridine to encourage non-neuronal cell elimination.[32]

Nerve Repair Preparation

TENGs were fabricated by stretch-growing DRG explants plated in custom-fabricated mechanical elongation bioreactors as previously described.[33-35] Briefly, DRGs were plated in two populations along the interface of an aclar "towing" membrane treated with poly-D-lysine (20 ug/mL) and laminin (20 µg/ml), resulting in a separation of approximately 500 µm. Cells were transduced with an AAV viral vector (AAV2/1.hSynapsin.EGFP.WPRE.bGH, UPenn Vector Core) to produce GFP expression in the neurons. At 5 days *in vitro* (DIV) the cells were incubated overnight in media containing the vector ($3.2x10^{10}$ genome copies/ml) and the cultures were rinsed with media the following day. Over 5 DIV, axonal connections were formed between the two populations. The populations were then gradually separated over the course of 6 days using a stepper motor system to displace the cells at a rate of 1 mm per day for 2 days and then 2 mm per day for 4 days, until the axons spanning them reached a total length of 1.0 cm as previously described (**Figure 1A-B**). Fresh, pre-warmed media was used to replace the culture media every 2-3 days. After 11-13 DIV, once the stretched constructs had reached the desired length, their health was assessed. Constructs appropriate for transplant were removed from the incubation chambers and embedded in a collagen-based matrix (80% v/v) in Minimum Essential Media (MEM 10X) and sterile cell culture grade water supplemented with NGF (2.5S, 0.05 ng/mL).[36] After gelation at 37°C, embedded cultures were gently removed and placed within a 1.2 cm long absorbable collagen nerve guidance tube (Stryker NeuroFlex™) and transplanted into a rat sciatic nerve injury model. For the NGT+DRG group, two populations of whole DRG explants (10 DRG in each row) were plated 1 cm apart on an ACLAR membrane to resemble the environment within the mechanobioreactor.[33-35] Axonal connections were allowed to form for 5 DIV as is done prior to initiation of mechanical tension for stretch grown constructs, and the cells were encapsulated

bioRxiv preprint doi: https://doi.org/10.1101/847988; this version posted November 20, 2019. The copyright holder for this preprint (which was not certified by peer review) is the author/funder. All rights reserved. No reuse allowed without permission.

in the collagen matrix described above and transferred into a 1.2 cm NGT for transplantation. The NGT control group received the same collagen matrix within the conduit.

Surgical Procedure

Nerve regeneration was evaluated *in vivo* in a 1 cm rodent sciatic nerve injury model at 2 weeks following injury. A total of 20 male Sprague-Dawley rats were assigned to 5 groups: naïve (n=5), autograft (n=3), nerve guidance tube (NGT) (n=4), NGT containing disorganized DRG neurons (NGT+DRG; n=4), and TENGs (n=4). In addition, a total of 10 naïve rats were used to validate the fluorescent retrograde tracing methodology compared to conventional immunohistochemistry. Rats were anesthetized with isoflurane and the left hind was cleaned with betadine. Meloxicam (2.0 mg/kg) was given subcutaneously and bupivacaine (2.0 mg/kg) was administered along the incision line subcutaneously. The gluteal muscle was separated to expose the sciatic nerve exiting the sciatic notch. The sciatic nerve was carefully dissected to its trifurcation. The sciatic nerve was sharply transected 5 mm distal to the musculocutaneous nerve and a 1 cm nerve injury was made. For autograft repairs, a reverse-autograft technique was used.[37] For NGT, NGT+DRG, and TENG repairs, the nerve stumps were carefully inserted into each end of the nerve guidance tube with an overlap of 1 mm, and the epineurium was secured to the tube using 8-0 non-absorbable prolene sutures. The NGT+DRG repair contained DRG neurons embedded in collagen and NGT repairs contained collagen only as described above. The surgical site was closed with 3-0 absorbable vicryl sutures and skin staples. Animals were recovered and returned to the vivarium.

Dye Application

At the terminal time point retrograde dye was applied to the nerve using a method previously described by Catapano et al.[38] In brief, a nerve cuff was fashioned by capping silicon tubing (A-M Systems, 807600, 0.058” x 0.077” x 0.0095”) with PDMS (Fisher Scientific, Sylgard) that was trimmed to a length of 4 mm. Nerve cuffs were stored in 70% ethanol until used. Prior to transplantation, the cuffs were rinsed in PBS and dried using a Kimwipe. In this study, retrograde dye transportation was evaluated following acute nerve regeneration at 14 days post repair. In a subset of animals, retrograde dye transportation was assessed following chronic nerve regeneration at 16 weeks post repair.

At 3 days after initial FR exposure, the surgical site was re-exposed and the sciatic nerve was harvested, 5 mm proximal to the repair zone and immersion-fixed in formalin. A 2 mm by 2 mm piece of Kim wipe was soaked in 30% Fluoro-Ruby (FR; EMD Millipore, AG335) and placed inside the capped silicon tube toward the bottom. The silicon cuff was compressed, thereby

bioRxiv preprint doi: https://doi.org/10.1101/847988; this version posted November 20, 2019. The copyright holder for this preprint (which was not certified by peer review) is the author/funder. All rights reserved. No reuse allowed without permission.

creating a negative pressure vacuum, and the cuff was placed at the face of the proximal nerve stump. By slowly releasing the compression on the tube, the negative press, re of the tube allowed for the sciatic nerve to seal into the tube. Tisseel Fibrin Sealant was applied around the cuff to fix the proximal nerve and cuff in place. (Baxter, 1504514). The surgical site was closed using 3-0 absorbable vicryl sutures and skin staples, and the animal returned to the vivarium for 3 days of FR exposure (**Figure 1C**).

Nerve Regeneration and Schwann Cell Infiltration Across the Repair Zone

Formalin-fixed, frozen nerve sections were rinsed in PBS (3x5 min) and blocked for 1 hour in blocking solution (PBS with 4% normal horse serum and 0.3% Triton X-100). Primary antibodies diluted in blocking solution were then applied and incubated overnight at 4°C. Mouse anti-phosphorylated neurofilament (SMI-31, 1:1000, BioLegend Cat# 801601) and mouse anti-nonphosphorylated neurofilament (SMI-32, 1:1000, BioLegend Cat# 701601) were used to identify axons; rabbit anti-S100 Protein Ab-2 (S100, 1:500, Thermo Scientific Cat# RB-044-A) was used to identify Schwann cells. Following incubation, slides were rinsed in PBS (3x5 min) and secondary antibodies prepared in blocking solution were applied for 2 hours at room temperature: donkey anti-mouse 568 (Alexa Fluor® 568, 1:500, Thermo Scientific Cat# A10037) and donkey anti-rabbit 647 (Alexa Fluor® 647, 1:500, Thermo Scientific Cat# A31573). Sections were then rinsed in PBS (3x5 min), mounted with Fluoromount-G® (Southern Biotech Cat#0100-01) and coverslipped. Images were obtained with a Nikon A1R confocal microscope (1024x1024 pixels) with a 10x air objective and 60x oil objective using Nikon NIS-Elements AR 3.1.0 (Nikon Instruments, Tokyo, Japan).

Spinal Cord Tissue Acquisition

Animals were transcardially perfused with 10% formalin and heparinized 0.9% NaCl. L4/L5 DRGs were extracted. Spinal cord T12-L6 region was extracted *en bloc*. All samples were fixed in paraformaldehyde overnight then placed in 30% sucrose for 48 hours. Full *en bloc* spinal cord was embedded in OCT then frozen. Tissue orientation was preserved with the use of tissue dye. Spinal cord samples were sectioned at 500 μm on a microtome cryostat and examined briefly under Nikon A1RSI Laser Scanning confocal microscope paired with NIS Elements AR 4.50.00 to screen sections with visible FR in the ventral horn. Spinal cord sections and DRGs with positive FR signal were stored in PBS for 24 hours.

Spinal Cord Optical Clearing

Spinal cords were sectioned into 500 μm thick blocks and DRGs were optically cleared using the Visikol method and all washes were conducted at 15-minute time intervals unless

bioRxiv preprint doi: https://doi.org/10.1101/847988; this version posted November 20, 2019. The copyright holder for this preprint (which was not certified by peer review) is the author/funder. All rights reserved. No reuse allowed without permission.

otherwise stated. Spinal cord sections were washed in increasing concentrations of methanol (50%, 70%, and 100%) and stored for 12 hours in 100% methanol. Samples were then exposed to 20% DMSO/methanol followed by decreasing concentrations of methanol (80% and 50%). Next, samples were washed with PBS followed by PBS/0.2% Triton X-100. Next, samples were incubated in penetration buffer (0.2% Triton X-100, 20% DMSO, and 0.3M glycine in 1X PBS), then blocking buffer (0.2% Triton X-100, 6% NHS, and 10% DMSO in 1X PBS) at 37°C for 19 hours each. Samples were rinsed twice in washing buffer, then exposed to primary antibodies (1:500 Rabbit NeuN) in antibody buffer (0.2% Tween, 10 µg/mL Heparin, 3% NHS, and 5% DMSO in 1X PBS). After incubation in primary antibodies, samples were rinsed ten times in washing buffer (0.2% Tween and 10 µg/mL Heparin in 1X PBS), followed by exposure to secondary antibodies (1:500 Donkey anti-rabbit 647). Samples were again rinsed ten times in washing buffer. Finally, samples were exposed to increasing concentrations of methanol (50%, 70%, and 100%) at three rinses each while incubated at 37 °C. The samples were then incubated in Visikol 1 for 24 hours, then Visikol 2 for 48 hours. For all DRG samples, these samples were placed in Visikol 1 after the initial ascending methanol steps.

Quantification of Ventral Horn and Dorsal Root Ganglia

For conventional immunohistochemistry: naïve spinal cords were harvested 3 days following FR application in order to validate the optical clearing technique. Briefly, samples were stored in 30% sucrose for 24 hours or until saturation for cryoprotection, embedded in OCT, and frozen in -80 µC isopentane. Axial sections were taken using a cryostat microtome (30 µm thick) and stained for NeuN (1:500 Rabbit NeuN, 1:500 donkey anti-rabbit 647). Slides were imaged at 20x using a Nikon A1RSI Laser Scanning confocal microscope paired with NIS Elements AR 4.50.00, taking z-stacks at 5 µm intervals. FR and NeuN cell counts were quantified from maximum projections. The Abercrombie correction for cell quantification was applied based on section thickness and an estimated cell size of 30 µm.[39]

For optical cleared tissue: samples were placed in glass bottom well plates and immersed fully in Visikol 2. Tissue was then imaged using Nikon A1RSI Laser Scanning confocal microscope under 10x air objective. All images were taken using a z-stack at 5 µm steps with laser settings optimized for naïve tissue. Images were analyzed using ImageJ FIJI software. Maximum projections of 100 µm were generated and all cells within the ventral horn (L4-L6) of the spinal cord and DRG (L4, L5) were quantified by drawing line ROI through background and the entirety of the cell body. Using a custom MATLAB script, the intensity value for each cell body was calculated with the following formula:

bioRxiv preprint doi: https://doi.org/10.1101/847988; this version posted November 20, 2019. The copyright holder for this preprint (which was not certified by peer review) is the author/funder. All rights reserved. No reuse allowed without permission.

$$\frac{maximum\ intensity - background\ intensity}{background\ intensity}$$

Functional Assessment

At 16 weeks post repair, compound muscle action potential (CMAP) was assessed to evaluate functional regeneration. Animals were re-anesthetized and the graft was re-exposed, and the nerve was stimulated and CMAPs were recorded from a bipolar subdermal electrode placed in the tibialis anterior (biphasic; amplitude: 0–10 mA; duration: 0.2 ms; frequency: 1 Hz) using a handheld bipolar hook electrode (Rochester Electro-Medical, Lutz, FL; #400900) 5 mm proximal to the repair zone. The supramaximal CMAP recording was obtained and averaged over a train of 5 pulses (100x gain and recorded with 10–10,000 Hz band pass and 60 Hz notch filters).

Statistical Analysis

For conventional and optical cleared quantification: the mean and standard error were calculated for cell counts and compared using a parametric one-way ANOVA with multiple comparisons. To compare the number of FR+ cells across each experimental group, a parametric ANOVA test with multiple comparisons was conducted with an alpha value of 0.05. The intensity of every cell per animal was log transformed to fit the naïve group data to a normal distribution. Frequency distributions for each experimental group were calculated with a bin length of 0.1 for MN and DRG. These frequency distributions were normalized by dividing each bin frequency by the experimental group sample size. The mean intensity of each animal was averaged, and experimental groups were compared using a nonparametric Kruskal-Wallis ANOVA with multiple comparisons. A linear regression was generated between number of FR+ cells and the transformed mean intensity value.

Results

Repair Zone Analysis

Longitudinal sections from rat sciatic nerve grafts were immunostained with SMI31/32 and S-100 to visualize axons and Schwann cells, respectively, similar to previous studies.[40] Axonal infiltration from the proximal region into the graft region was observed across all groups (**Figure 2A-C, Figure 3**). Regenerating axons and Schwann cell infiltration were observed at higher magnification in longitudinal sections of the graft region. Diminished axon regeneration and Schwann cell infiltration was found compared to autograft, NGT+DRG, or TENG groups. Transplanted DRG expressing GFP survived transplantation in the NGT+DRG group (**Figure 2C**). Moreover, TENG neurons survived transplantation and extended axons into the distal nerve, and

bioRxiv preprint doi: https://doi.org/10.1101/847988; this version posted November 20, 2019. The copyright holder for this preprint (which was not certified by peer review) is the author/funder. All rights reserved. No reuse allowed without permission.

integrated with host Schwann cells and axons, enabling axon-facilitated axonal regeneration across the graft zone. (**Figure 3**).

Neuronal Labeling Validation in Optically Cleared Sections

To validate the optical clearing technique, FR and NeuN were visualized in 500 μm thick naïve spinal cord blocks. FR labeled cells were clearly visualized within optically cleared spinal cord stained for NeuN in both axial and longitudinal blocks and adequate antibody penetration was confirmed in the volumetric reconstruction of the Z-stack images across various X-Y-Z planes **(Figure 4**). FR and NeuN cells were quantified in maximum projection z-stack images for 500 μm thick sections of spinal cords and 30 μm thick frozen sections. Conventional IHC cell counts were significantly higher for FR and NeuN counts than the IHC quantification with the Abercrombie correction (IHC+AC) or Visikol HISTO sectioning. No statistical significance was found for FR or NeuN quantification between the IHC+AC and Visikol HISTO methods ($p > 0.05$; **Figure 5**).

Ventral Horn Retrograde Labeling Analysis

TENG repairs exhibited a similar number of FR+ labelled MN neuronal bodies (1038.0 ± 100.5) as naïve (935.0 ± 35.4) and autograft repairs (914.7 ± 35.4) ($p > 0.05$). TENG repairs also exhibited a significant increase from NGT (357.3 ± 52.3, $p < 0.001$) and NGT+DRG repairs (678.8 ± 82.6, $p < 0.05$). NGT repairs exhibited a significantly decreased number of FR+ labelled neuronal cell bodies as compared to naïve, autograft and TENG repairs ($p < 0.001$). NGT+DRG repairs produced a significant increased improvement in FR+ cell counts as compared to NGT repair ($p < 0.05$) (**Figure 6**). NeuN were also quantified within the ventral horn of the spinal cord. NGT NeuN counts were significantly less than naïve and autograft NeuN counts ($p < 0.05$) while NGT+DRG and TENG NeuN counts were not statistically different from other experimental groups ($p > 0.05$) (**Figure 6)**. The intensity of FR uptake per neuron was also quantified as a further metric of neuronal health. We found a positive correlation between number of FR+ cells and the mean intensity of those cells ($y = 0.0005071x - 0.628$; $R^2 = 0.417$) (**Figure 7)**. Also, the distribution of FR intensity per cell most closely matched the naïve group for autograft and TENG repairs (**Figure 7**).

Dorsal Root Ganglia Retrograde Labeling Analysis

No statistical difference was found in the number of FR+ cells across experimental groups in the L4 and L5 DRG regions (**Figure 8**). The intensity of FR uptake per neuron was again quantified as a metric of neuronal health. A positive correlation between number of FR+ cells and the mean intensity of those cells was observed, although the correlation was weaker than that found with MNs ($y = 0.000109x - 0.00565$; $R^2 = 0.230$) (**Figure 9**). The distribution of FR intensity

bioRxiv preprint doi: https://doi.org/10.1101/847988; this version posted November 20, 2019. The copyright holder for this preprint (which was not certified by peer review) is the author/funder. All rights reserved. No reuse allowed without permission.

per cell most closely matched the naïve group following autograft repairs, with the distribution following TENG repairs being more similar to naïve that the NGT or NGT+DRG repairs (**Figure 9**).

FR Uptake and Functional Assessment at 16 Weeks Post Repair.

Qualitative assessment of a subset of animals at 16 weeks post repair revealed similar number of labeled spinal motor neurons following TENG and autograft repair, as compared to a reduced number of labeled neurons following NGT repair (**Figure 10**). No differences were observed in the labeling of DRG neurons between groups. CMAP recordings were obtained in all animals at 16 weeks post repair; however, the amplitude of the response was consistently much greater following TENG or autograft repair than following NGT repair.

Discussion

PNI recovery is a race against time since regenerating axons have a limited period to reach distal end targets before the pro-regenerative distal nerve environment loses its capacity to support regeneration. Many grafts have been developed to facilitate nerve regeneration and sustain a pro-regenerative environment in the distal segment.[33,41-46] However, there has been limited focus on the ability for a graft to influence the intrinsic regenerative capacity of the proximal neuron. To the best of our knowledge, this is the first study to investigate the effect of different peripheral nerve repair strategies on the proximal neuron health and regenerative capacity.

In this study, FR uptake in the host spinal cord and DRG was quantified as a surrogate marker for retrograde transport and overall neuron health. At 2 weeks post repair, a similar number of FR+ cells were found in the ventral horn between TENG, autograft, and naïve groups. Contrastingly, the NGT repair group had nearly 30% fewer FR+ neurons, likely due to lack of neurotrophic and anisotropic structural support. Furthermore, the average fluorescent intensity of the FR+ cells in the NGT repair group were significantly less than the autograft or naïve groups. Nerves repaired with NGTs seeded with disorganized DRG populations exhibited a slight increased level of retrograde transport compared to the NGT group, potentially indicating the benefit of a cellular trophic component in a PNI graft. The benefit of a living component in a nerve graft was further corroborated with Schwann cell proliferation surrounding transplanted cells within the graft zone. Although the difference in FR+ labeling in the ventral spinal cord of NGT and NGT+DRG groups indicates cellular advantage, FR+ cells labeled in the NGT+DRG group were unable to effectively sustain retrograde transport to levels seen in TENG or autograft repairs.

bioRxiv preprint doi: https://doi.org/10.1101/847988; this version posted November 20, 2019. The copyright holder for this preprint (which was not certified by peer review) is the author/funder. All rights reserved. No reuse allowed without permission.

This potentially indicates the dual importance in a PNI nerve graft that supplies trophic factors while simultaneously taking advantage of biomimetic structural organization.

Additionally, the number of NeuN cells in the spinal cord were similar between naïve animals and following repair with TENG or NGT+ DRG. Contrastingly, NGT repairs exhibited a significant loss of NeuN-labeled spinal motor neurons. Although previous studies have shown that chronic nerve axotomy can lead to a rapid and persistent loss of NeuN expression in the spinal cord ventral horn, it is not well-characterized with respect to different repair strategies.[47] For example, crush injury has been reported to result in a transient reduction of NeuN expression that ultimately returns to normal following regeneration.[48] Therefore, at the acute time point following segmental nerve repair reported in our study, the loss of NeuN expression is likely transient during the regenerative process. Indeed, decreased NeuN expression likely does not necessitate permanent neuronal cell death; rather, it is an indicator of neuronal cell health. Although the decreased NeuN expression may be transient, these findings potentially imply that there are a large number of unhealthy proximal neurons during a crucial period for regeneration. Moreover, the ability for living scaffolds to sustain neuronal health at an acute time point further suggests the importance for maintaining overall regenerative capacity.

Although there were stark differences in the level of FR and NeuN expression in the ventral spinal cord, there did not appear to be any significant change in DRG neurons based on FR or NeuN expression across experimental groups. These results are consistent with previous studies that found no change in number of retrogradely labeled DRG neurons at two weeks following sural nerve axotomy.[49] Previous studies additionally corroborate this finding, demonstrating that sensory neurons are more resilient and regenerate more robustly than motor neurons at early timepoints following nerve axotomy.[50,51] However, more extensive studies are necessary to elucidate any differences in DRG.

In this study, retrograde transport was used as a corollary marker for neuronal cell health. Nerve regeneration has been studied from a multi-faceted approach, most commonly through electrophysiological tests.[52] However, given the importance of protein synthesis and transportation with neuronal cell health, active retrograde transport is strongly implicated as a marker for regenerative capacity.[53] While there is substantial evidence that retrograde transport is modulated through varying levels of neuronal cell helath,[14] other mechanisms, such as the rate of axonal resealing, might modulate the amount of FR transported to the neuronal cell body.[54,55] Previous studies have shown evidence that axon diameter may also influence rate of microtubule-based retrograde transport.[56,57] In order to conclusively implicate active retrograde transport as the modulator of observed changes in FR expression, it may be of interest in future experimental

bioRxiv preprint doi: https://doi.org/10.1101/847988; this version posted November 20, 2019. The copyright holder for this preprint (which was not certified by peer review) is the author/funder. All rights reserved. No reuse allowed without permission.

designs to include a control repair group that is exposed to a retrograde transport inhibitor, such as Ciliobrevin D.[58,59]

Living scaffolds provide a bolus of pro-regenerative neurotrophic factors that supports regenerating axons and ultimately enables functional recovery. In this study, we found TENGs and autografts had a similar degree of healthy neurons at an acute time period and functional recovery chronically as compared to NGTs. Future studies are necessary to further investigate whether early recovery of neuronal health also improves the capacity for muscle reinnervation. To understand regenerative capacity further for clinical applicability, future studies might include additional cell markers to provide additional insight into the neurons that are actively regenerating toward the end targets. The varying expression profile of certain transcriptional factors, such as ATF-3 and C-JUN, following nerve injury, during regeneration, and until reinnervation could be combined with FR expression data to provide greater insight into the duality between regeneration and neuronal cell health.[60-63]

Although TENGs have demonstrated the potential for preserving neuronal cell health, further optimization is necessary to tailor the repair strategy for specific injuries. For example, sensory nerve autografts are typically used to repair all injuries, including primarily motor as well as mixed motor-sensory nerves. Recently, there has been some evidence that motor nerve autografts increase functional recovery.[64] Therefore, it might be useful to develop modality-specific TENGs comprised of sensory, motor, or mixed motor-sensory neurons/axons to further enhance the regenerative capacity.[65] However, in this study, TENGs comprised of DRG neurons/axon tracts appeared to maintain neuronal cell health in MN regions of the spinal cord.

To date, the only current commercially available NGTs are empty conduits which lack neurotrophic and anisotropic support. Numerous previous studies have reported repairs with a NGT resulted in diminished functional recovery compared to an autograft repair, even in gap repairs less than 1.5 cm.[66,67] Our study corroborated this by demonstrating that an acellular graft with solely structural isotropic support from collagen was unable to support cell survival and regenerative capacity as compared to other grafts. NGTs are therefore inadequate clinical vessels for supporting effective, healthy, and functional regeneration. Acellularized nerve allografts (ANAs) were developed as an alternative non-living scaffold repair strategy that provided regenerating axons with the nerve architecture and haptic cues similar to an autograft repair.[68,69] However, ANAs lack a cellular component and the necessary trophic support for sustained nerve regeneration, thus likely minimizing the regenerative capacity and functional recovery.[70]

bioRxiv preprint doi: https://doi.org/10.1101/847988; this version posted November 20, 2019. The copyright holder for this preprint (which was not certified by peer review) is the author/funder. All rights reserved. No reuse allowed without permission.

Recent studies have developed biomimetic smart materials to offer a counter argument to acellular nerve guidance tubes by adding biological components and proteins, such as extracellular matrix, NGF, BDNF, and GDNF.[71-78] These boosted grafts, may prove effective in some instances of neural regeneration, including sustainment of host neurons during long distance gap repairs.[79,80] However, despite these novel engineering feats, even with the addition of biological fillers, acellular grafts remain unable to address overall shortcomings in nerve regeneration.[81] Often, undesirable results have been reported using "smart materials", such as "the candy store effect". This effect is observed following the supplementation of a nerve guidance tube with exogenous GDNF. Rather than promoting nerve regeneration with a strong chemoattractant for regenerating axons, the neurite outgrowth migrates to the site of the GDNF and does not move past this site of application – effectively countering the intended process of regeneration.[82,83] As our data demonstrated, even by supplementing NGTs with disorganized DRGs, likely capable of relaying helpful signals to regenerating axons, they were still unable to provide the necessary structure for maintenance of motor neuron cell health. Just as a solely structural advantage to a graft is not enough for maximal regenerative capacity, a solely living component with no structural anisotropic arrangement appears to also be insufficient. For this reason, autografts remain the only living scaffold strategy currently available in a surgeon's armamentarium for peripheral nerve reconstruction that provides regenerating axons with native architecture and the cellular support necessary for sustaining neuronal survival.[66] However, autografts have inherent shortcomings, including donor site morbidity and limited availability of donor nerve for long-gap nerve repair and/or polytrauma resulting in multiple nerve injuries. Cell transplantation within NGTs are able to provide neurotrophic support with *in vivo* feedback loops have demonstrated some initial promise in short-gap, long-gap, and delayed nerve repairs.[84,85] However, in cases of cell transplantation, the host immune response should be considered.[86,87]

TENGs have continued to demonstrate the potential to overcome major limitations in current NGT technology. Our group has previously reported that TENGs result in axon-facilitated axonal regeneration and maintenance of the pro-regenerative distal pathway support architecture.[88] TENG axons penetrate the host distal segment and "babysit" the distal Schwann cells as host regenerating axons cross the segmental defect. In the current study, we have shown TENGs also preserve the regenerative capacity of the proximal neuronal populations within the spinal cord, thereby potentially increasing the ceiling for host regeneration and functional recovery (**Figure 11**). In this study, TENG repairs resulted in a greater number of motor neurons maintained following PNI as compared to the NGT. In fact, within these motor neuron regions of the spinal cord, TENGs preserved FR and NeuN expression comparable to autografts. Furthermore, we

bioRxiv preprint doi: https://doi.org/10.1101/847988; this version posted November 20, 2019. The copyright holder for this preprint (which was not certified by peer review) is the author/funder. All rights reserved. No reuse allowed without permission.

have found a dramatic reduction in neuronal cell health observed with NGT repairs, which has been corroborated by clinical reports demonstrating poor functional recovery.[77,89] As such, we propose future work is necessary to further understand the importance of proximal neuron preservation for functional recovery (**Figure 11**). As a living scaffold, TENGs represent a promising technology that preserves the regenerative capacity following repair and ultimately increase the ceiling for functional recovery.

bioRxiv preprint doi: https://doi.org/10.1101/847988; this version posted November 20, 2019. The copyright holder for this preprint (which was not certified by peer review) is the author/funder. All rights reserved. No reuse allowed without permission.

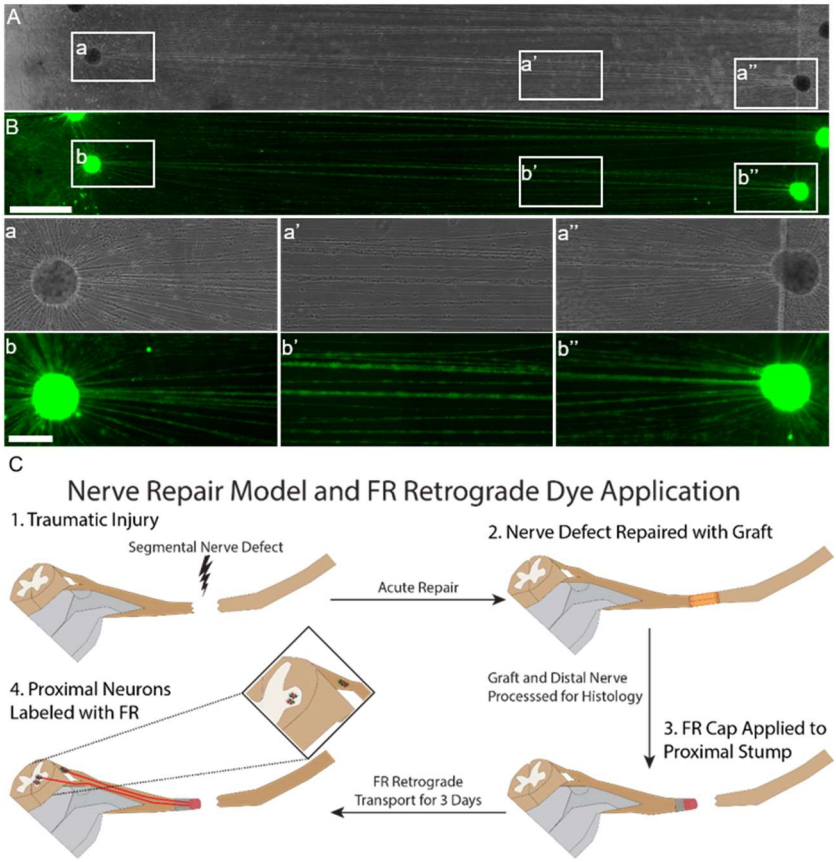

Figure 1. Micrographs of Neuron Populations Following "Stretch-Growth and Concept for Nerve Repair Model and Fluoro-Ruby (FR) Retrograde Fluorescent Dye Application. Embryonic rat GFP+ DRG explants were plated on a towing membrane and allowed to integrate *in vitro*. The axons were subjected to "stretch-growth" in custom mechanobioreactors. (A-B) Example of two DRG populations that were stretched to 1 cm for transplantation in phase in (A) phase contrast and (B) and fluorescent microscopy. (C) In this study, a retrograde fluorescent dye (FR) was applied at 2 weeks following a 1 cm rodent segmental nerve repair proximal to the graft site, and the nerve was harvested for histological analysis. At 3 days post application, the animal was euthanized and the spinal cord and DRG were harvested for histological analyses. Scale bar 100 μm.

bioRxiv preprint doi: https://doi.org/10.1101/847988; this version posted November 20, 2019. The copyright holder for this preprint (which was not certified by peer review) is the author/funder. All rights reserved. No reuse allowed without permission.

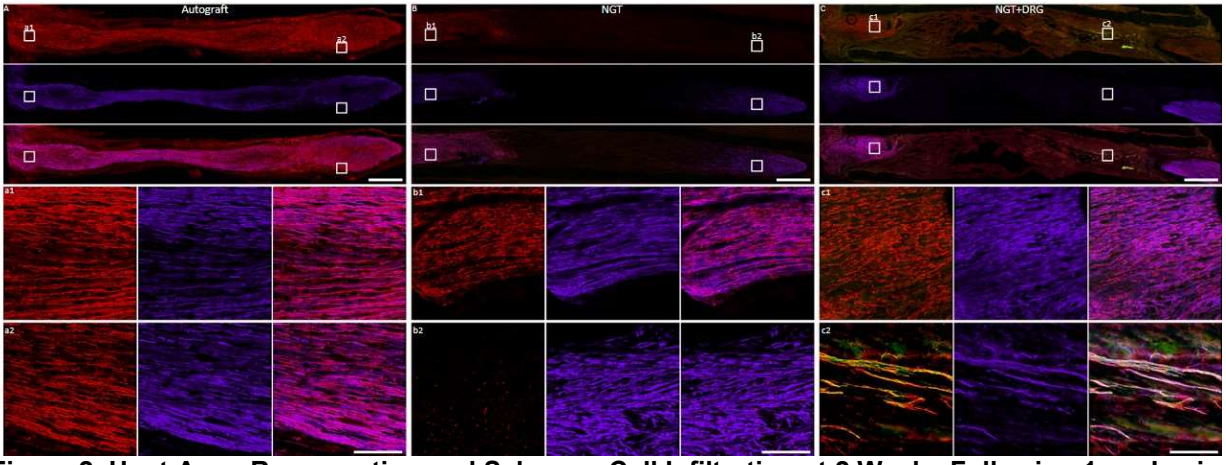

Figure 2. Host Axon Regeneration and Schwann Cell Infiltration at 2 Weeks Following 1 cm Lesion in Rat Sciatic Nerve. Confocal reconstruction of longitudinal frozen sections (20 μm) of rat sciatic nerve following autograft repair (A), NGT repair (B), and NGT+DRG repair (C). Higher magnification images (a-c) showing sections labeled for regenerating axons (SMI31/32+) and Schwann cells (S100). Transplanted DRG neurons expressing GFP can be observed in the NGT-DRG group (C). Many axons crossed the graft region following autograft repair (A). Axon ingrowth and Schwann cell infiltration were attenuated following NGT repair (B). Transplanted DRG survived and facilitated improved host axon ingrowth (C). Scale: A-D 1000 μm; a-d 100 μm.

bioRxiv preprint doi: https://doi.org/10.1101/847988; this version posted November 20, 2019. The copyright holder for this preprint (which was not certified by peer review) is the author/funder. All rights reserved. No reuse allowed without permission.

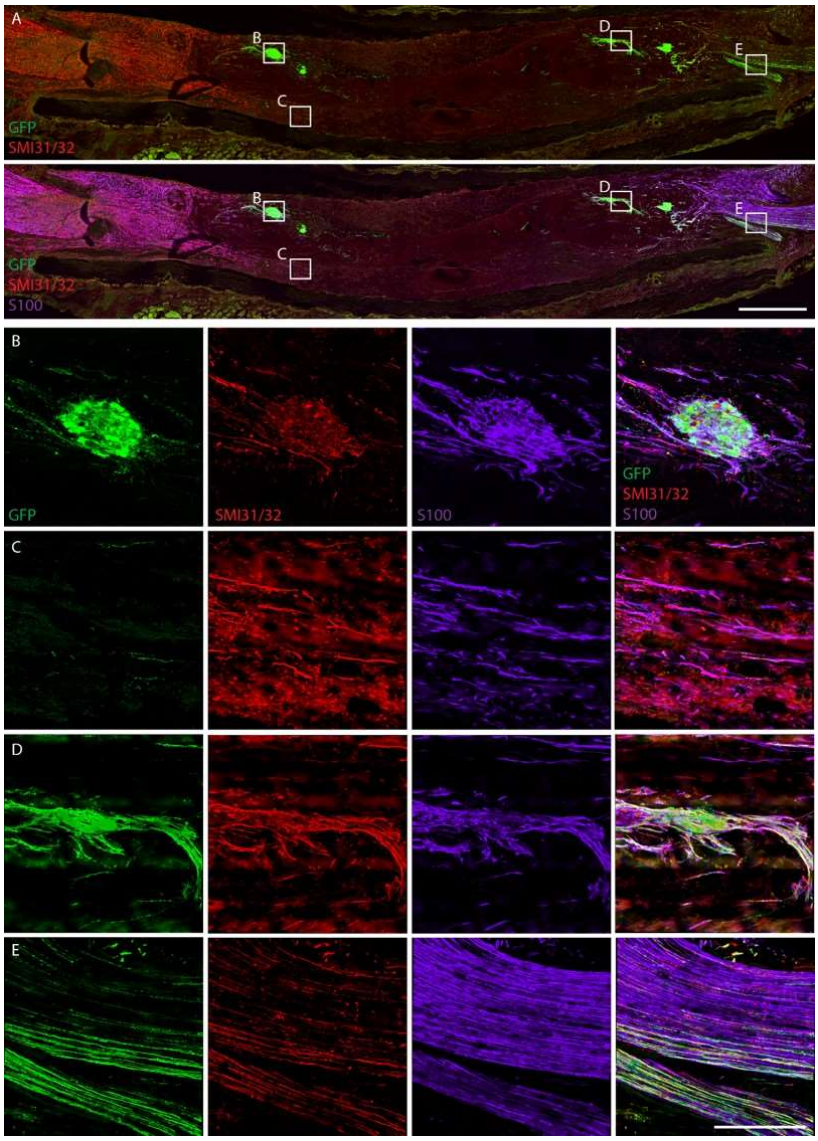

Figure 3. TENG Neuron-Axon Survival, Facilitation of Host Axonal Regeneration, and TENG Axon Extension into Distal Nerve. Confocal reconstruction of longitudinal frozen sections (20 μm) of rat sciatic nerve lesion (1 cm) at 2 weeks following TENG repair labeled to denote TENG neurons and axons (GFP+), host Schwann cells (S100+) and axons (SMI31/32+) (A). Higher magnification images reveal TENG neuronal survival post-transplantation (B,D) and integration with host Schwann cells and axons (B,D). This corresponded with host axon regeneration across the graft zone (C) and extending into the distal nerve along with TENG axons (E). Scale: A 1 mm; B-E 100 μm.

bioRxiv preprint doi: https://doi.org/10.1101/847988; this version posted November 20, 2019. The copyright holder for this preprint (which was not certified by peer review) is the author/funder. All rights reserved. No reuse allowed without permission.

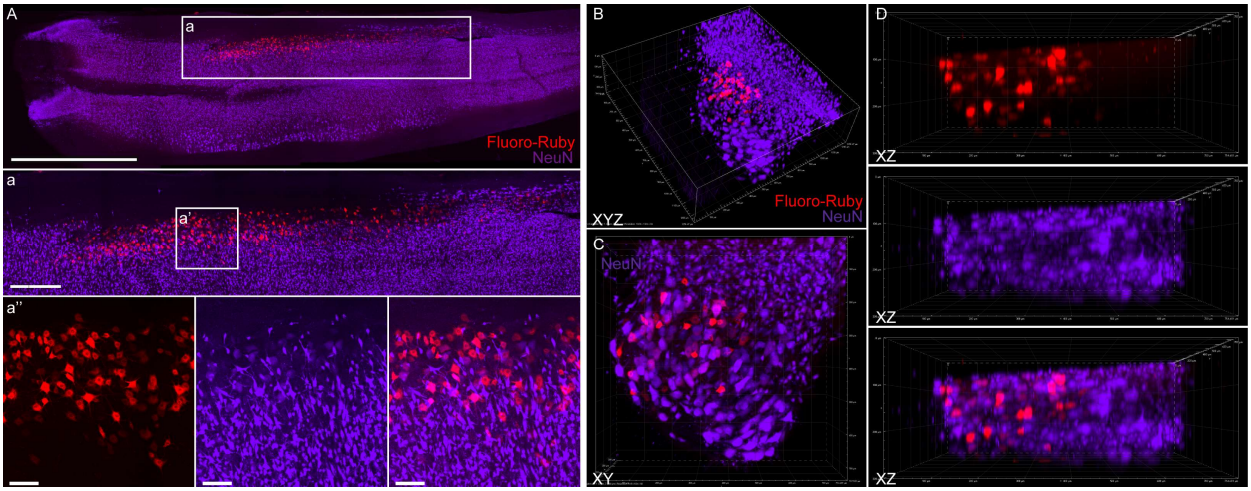

Figure 4. Optically-Cleared Spinal Cord Stained for NeuN Enables Visualization of FR-Labeled Neurons. Visikol HISTO protocol can be used to analyze spinal cord tissue longitudinally or axially in 500 µm thick macro sections. (A) Fluoro-Ruby labelled cells and NeuN immunostained cells can be visualized in maximum projection z-stacks. Scale bars: 3000 µm, 600 µm, 60 µm. (B) Visual confirmation of sufficient NeuN antibody penetration and laser penetration through entirety of the 3D confocal reconstruction. XYZ view of axial spinal cord ventral horn section labelled with Fluoro-Ruby and NeuN. (C) XY 3D view of axial spinal cord ventral horn section. (D) XZ view of axial spinal cord section, confirming sufficient laser penetration to view Fluoro-Ruby through entirety of section.

bioRxiv preprint doi: https://doi.org/10.1101/847988; this version posted November 20, 2019. The copyright holder for this preprint (which was not certified by peer review) is the author/funder. All rights reserved. No reuse allowed without permission.

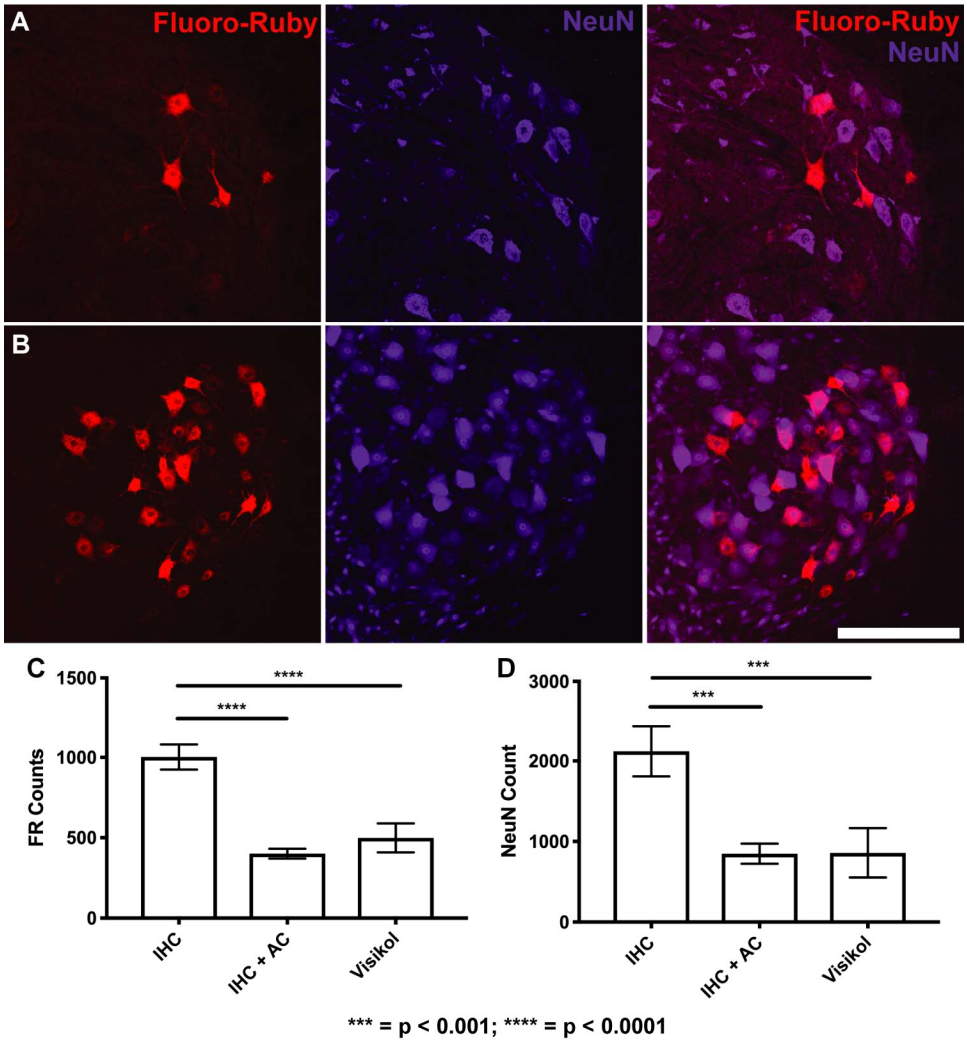

Figure 5. FR and NeuN Quantification in Naïve Spinal Cord Tissue to Validate Optical Clearing Technique with Conventional IHC Methodology. (A) Standard IHC (30 µm histological samples), z-stack maximum projection. (B) Spinal cord tissue blocks (500 µm sections) stained for NeuN IHC during Visikol HISTO process, z-stack maximum projection. Scale bar: 300 µm. (C) No statistical significance was found following quantification of sections stained using conventional IHC in standard 30 µm histological samples, with Abercrombie correction (IHC+AC) or Visikol cleared tissue. Error bars represent standard deviation.

bioRxiv preprint doi: https://doi.org/10.1101/847988; this version posted November 20, 2019. The copyright holder for this preprint (which was not certified by peer review) is the author/funder. All rights reserved. No reuse allowed without permission.

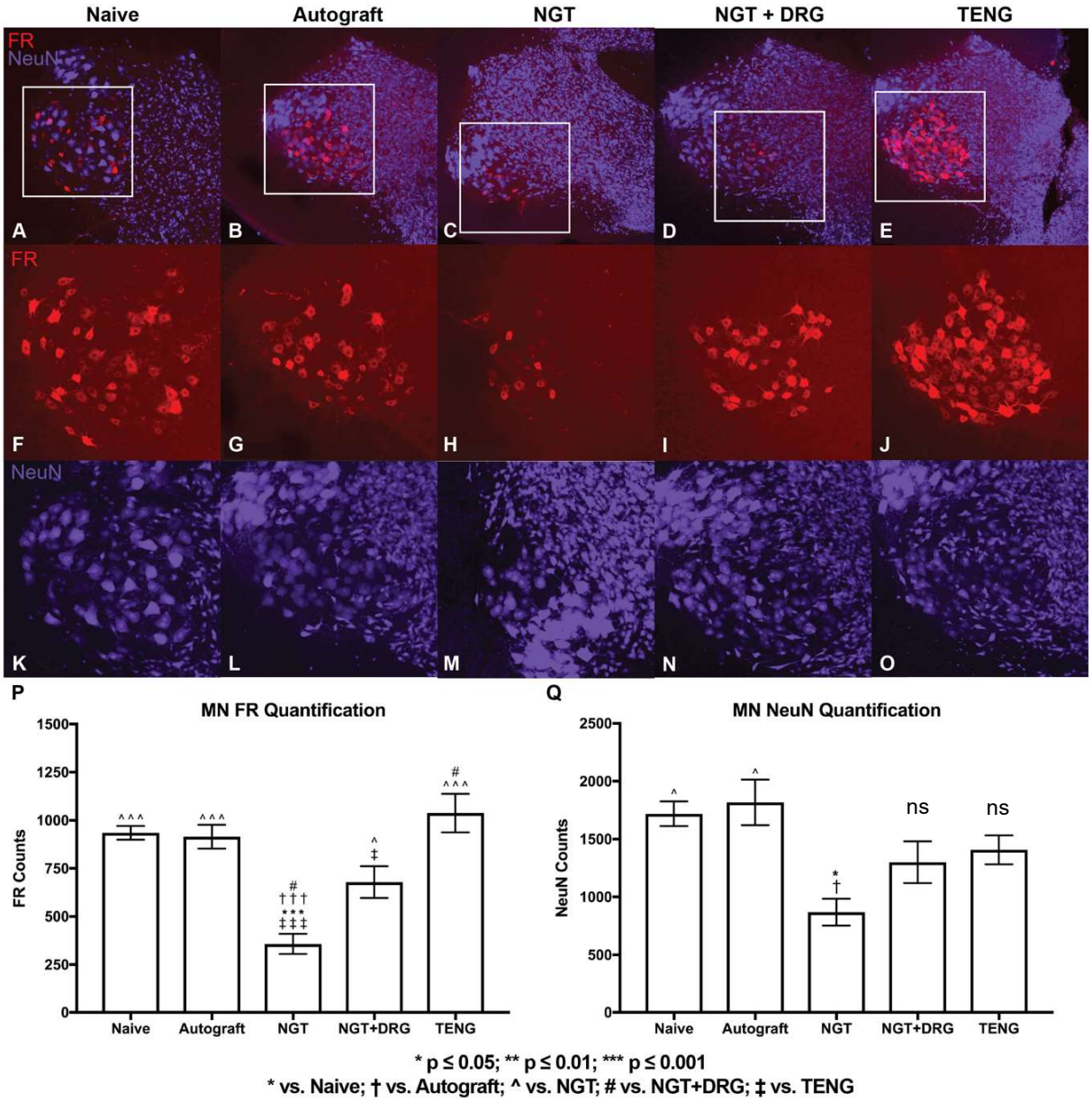

Figure 6. FR Retrograde Tracing and MN Quantification in the Ventral Horn Spinal Cord. MN cell bodies labeled with FR and NeuN were visualized in the ventral horn of optically cleared spinal cords (A-O). FR+ MN cell bodies in the ventral horn were quantified (P). When compared with naïve, both NGT ($p < 0.0001$) and NGT+DRG ($p < 0.05$) repair strategies produced a statistically significant difference in mean count. NeuN cell bodies were quantified in the ventral horn and a statistical difference was observed between the naïve and NGT repair strategies ($p < 0.05$) (Q). Scale bar: 200 μm. Error bars represent SEM. ns denotes no significance compared to naïve.

bioRxiv preprint doi: https://doi.org/10.1101/847988; this version posted November 20, 2019. The copyright holder for this preprint (which was not certified by peer review) is the author/funder. All rights reserved. No reuse allowed without permission.

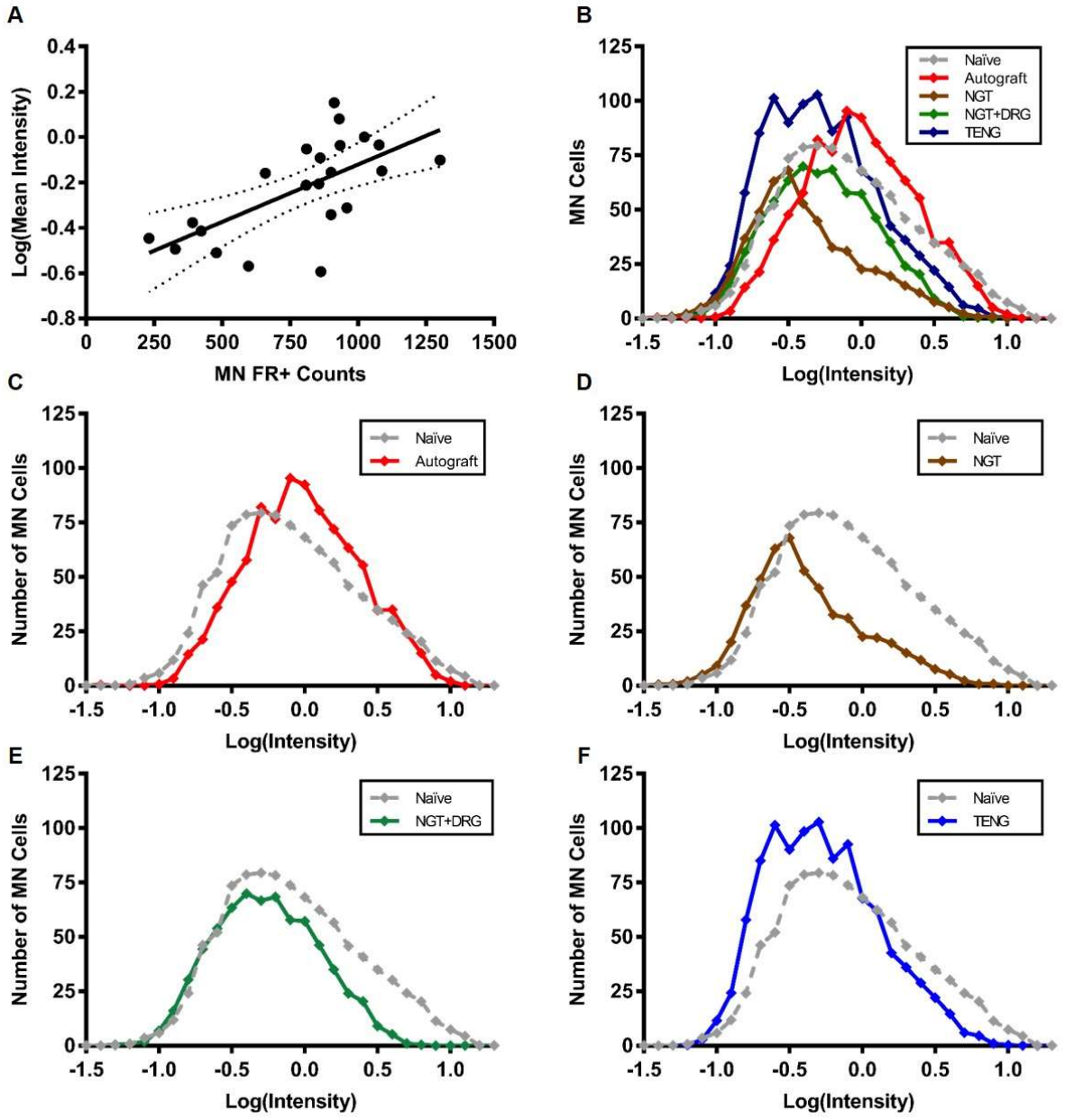

Figure 7. FR Intensity in Ventral Horn Motor Neuron Population. Intensity of FR fluorescence was calculated for each FR+ cell using maximum intensity of the cell and the background of the cell. Individual cell intensity was log transformed to fit a normal distribution. A linear regression model of mean intensity and total FR+ count was generated. Dashed lines represent SEM (A). Frequency distributions of DRG fluorescence intensity were plotted (B). Frequency distributions for each experimental group were compared to the naïve frequency distribution (C-F).

bioRxiv preprint doi: https://doi.org/10.1101/847988; this version posted November 20, 2019. The copyright holder for this preprint (which was not certified by peer review) is the author/funder. All rights reserved. No reuse allowed without permission.

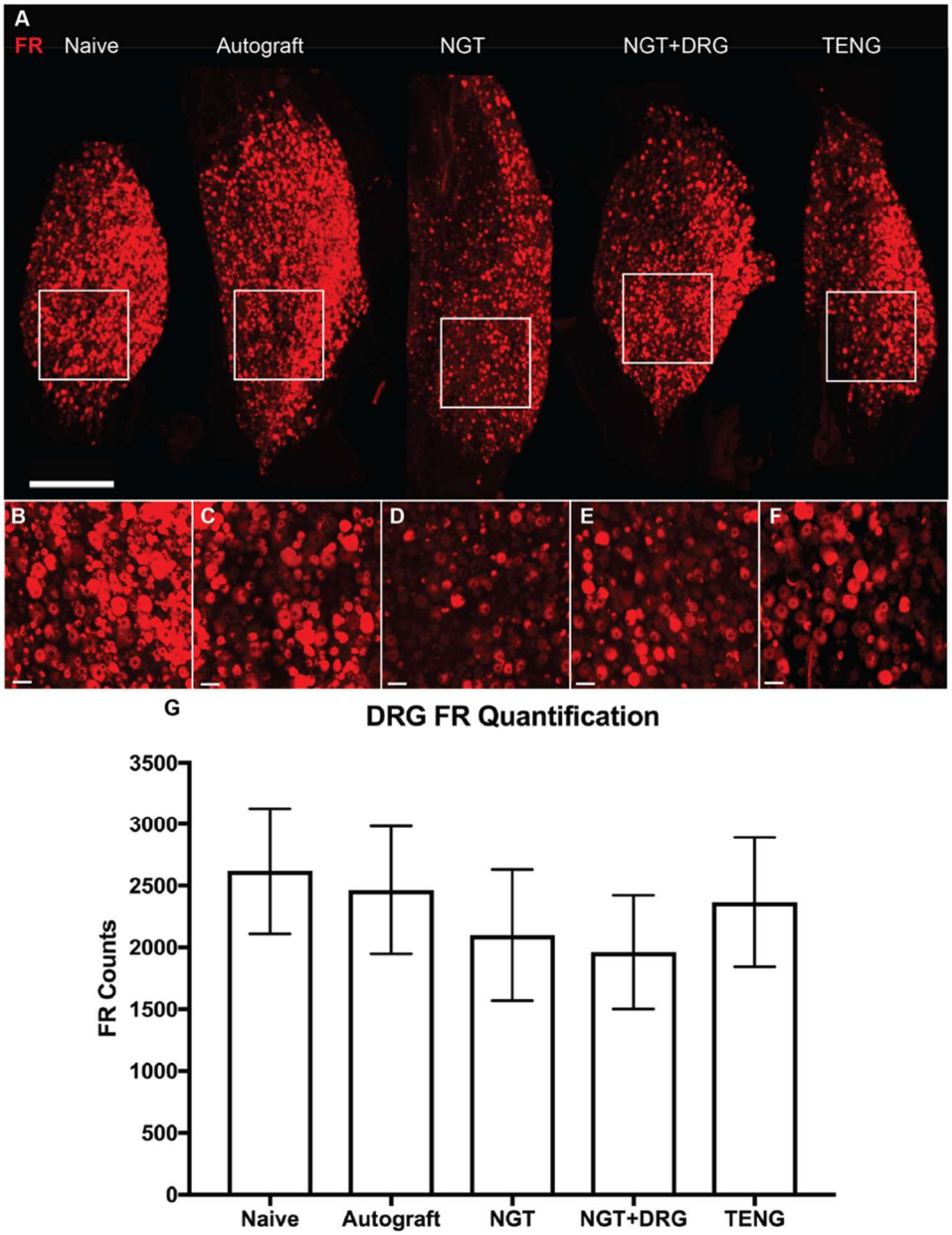

Figure 8. FR Quantification in L4 and L5 DRG. L4/L5 DRG samples were visualized *en bloc* following whole mount optical tissue clearance (A). FR+ DRG cell bodies were quantified. No statistical difference was observed between any treatment group for L4/L5 DRG FR counts (B,C). Error bars represent SEM. Scale bar: 700 µm.

bioRxiv preprint doi: https://doi.org/10.1101/847988; this version posted November 20, 2019. The copyright holder for this preprint (which was not certified by peer review) is the author/funder. All rights reserved. No reuse allowed without permission.

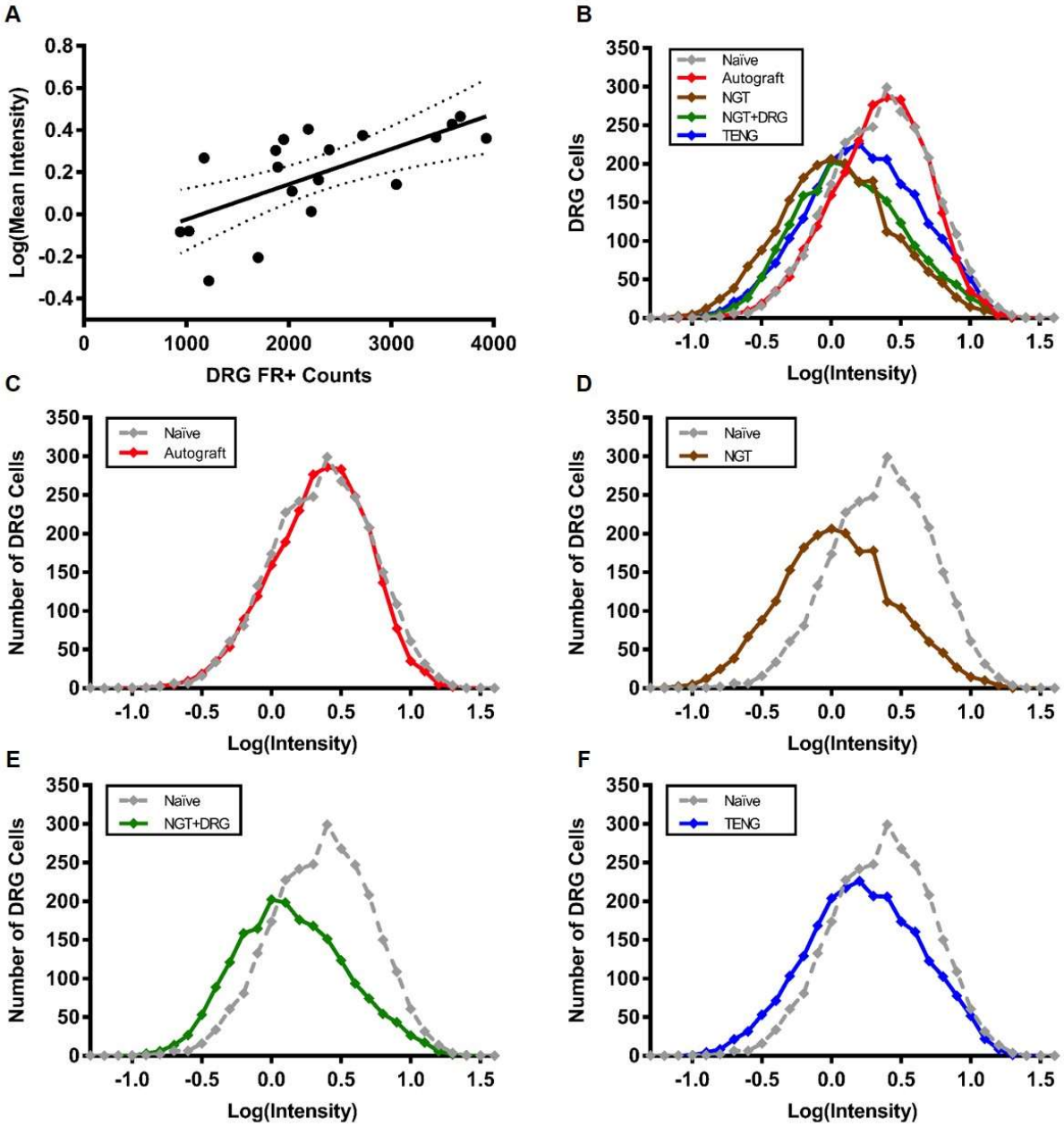

Figure 9. FR Intensity in L4 DRG. Mean intensity of FR fluorescence was calculated and a linear regression model of mean intensity and total FR+ count was generated. Dashed lines represent SEM (A). Frequency distributions of DRG fluorescence intensity were plotted (B). Frequency distributions for each experimental group were compared to the naïve frequency distribution (C-F).

bioRxiv preprint doi: https://doi.org/10.1101/847988; this version posted November 20, 2019. The copyright holder for this preprint (which was not certified by peer review) is the author/funder. All rights reserved. No reuse allowed without permission.

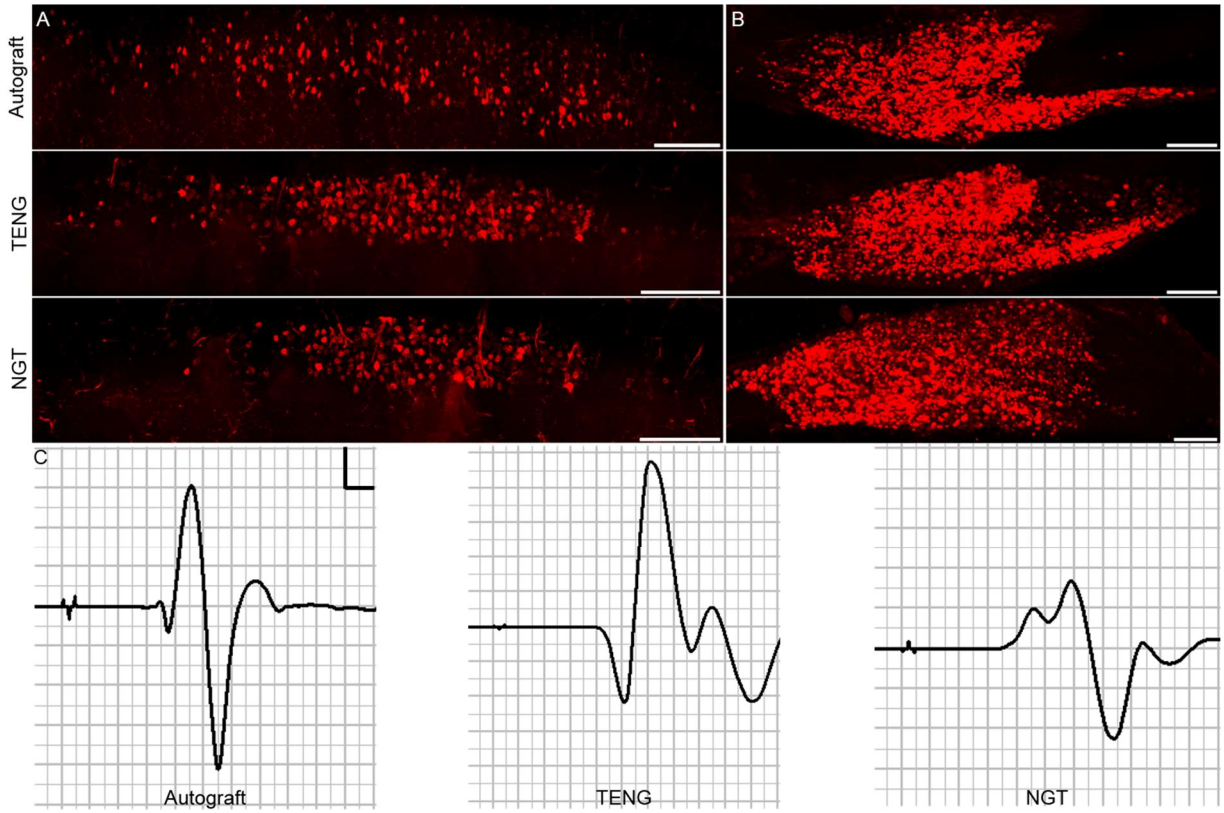

Figure 10. FR Uptake in Spinal Motor Neurons and DRGs at 16 Weeks Post Repair. In a subset of animals, (A) spinal motor neurons and (B) DRGs were labeled with FR at 16 weeks following peripheral nerve repair. Qualitative assessment revealed similar number of labeled spinal motor neurons following TENG and autograft repair and no differences were observed in the DRG between groups. (C) Similar muscle electrophysiological recovery was observed between the TENG and AG repair groups. Scale bar: 100 μm, 0.1 mv/0.1 ms.

bioRxiv preprint doi: https://doi.org/10.1101/847988; this version posted November 20, 2019. The copyright holder for this preprint (which was not certified by peer review) is the author/funder. All rights reserved. No reuse allowed without permission.

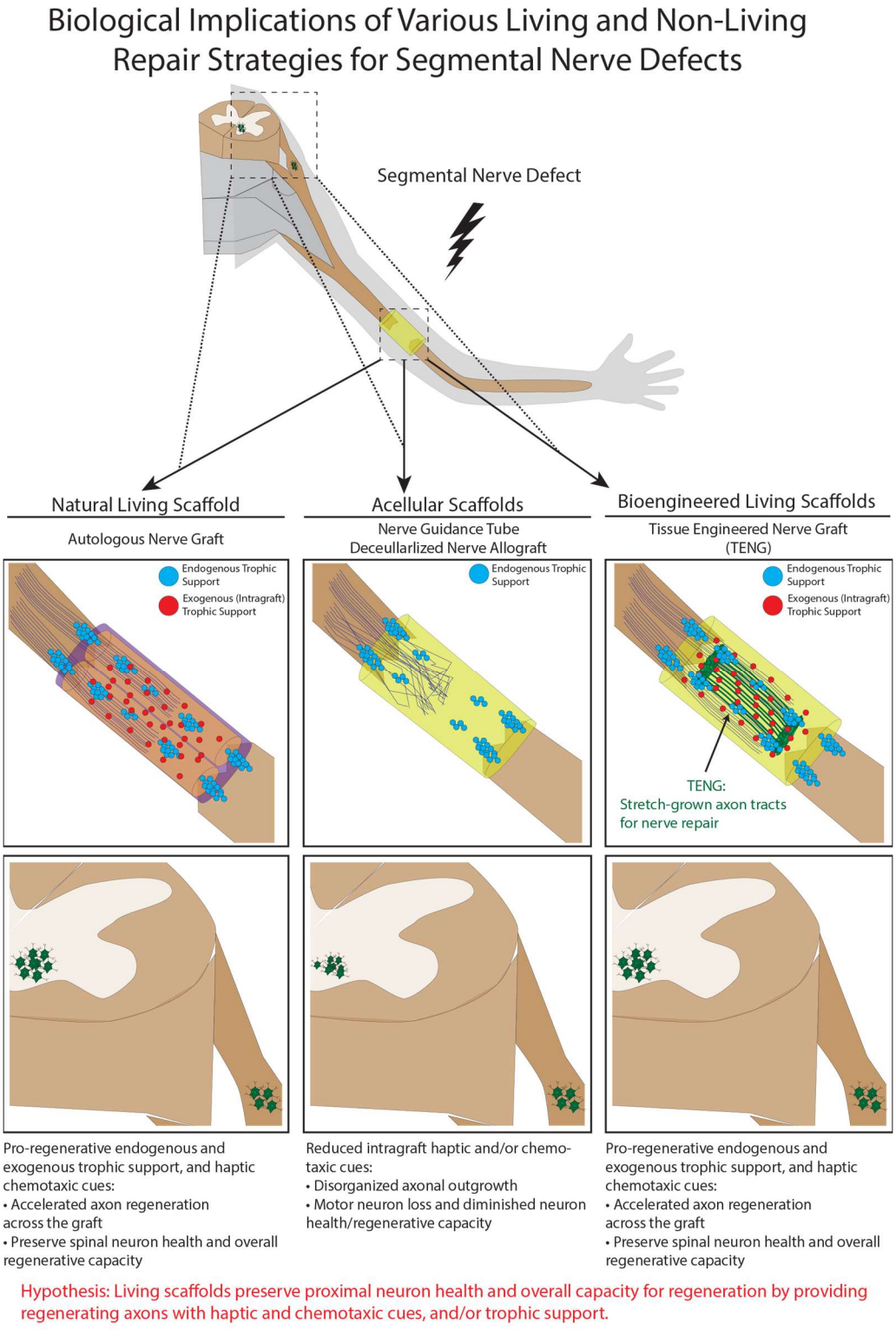

Figure 11. Biological Implications of Various Living and Non-Living Repair Strategies for Segmental Nerve Defects

bioRxiv preprint doi: https://doi.org/10.1101/847988; this version posted November 20, 2019. The copyright holder for this preprint (which was not certified by peer review) is the author/funder. All rights reserved. No reuse allowed without permission.

Author Contributions

D.K.C. conceived the study and provided the experimental design. K.S.K. fabricated the TENGs. J.C.M. and J.C.B. performed the surgeries. K.D.B. provided critical perspective on surgical paradigm and outcome measures. J.C.M., J.C.B., F.A.L., and K.D.B. conducted the histological assessments and analyses. J.C.M., J.C.B., and F.A.L. assisted with figure preparation. J.C.M., J.C.B., and D.K.C. prepared the manuscript. All authors provided critical feedback on the manuscript.

Competing Financial Interests

D.K.C is a co-founder and K.S.K. is currently an employee of Axonova Medical, LLC, which is a University of Pennsylvania spin-out company focused on translation of advanced regenerative therapies to treat nervous system disorders. Multiple patents relate to the composition, methods, and use of tissue engineered nerve grafts, including U.S. Patent 9,895,399 (D.K.C.), and U.S. Provisional Patent 62/569,255 (D.K.C). No other author has declared a potential conflict of interest.

Acknowledgements

The authors would like to thank Michael Johnson and Tom Villani of Visikol for technical support. Financial support provided by the U.S. Department of Defense [CDMRP/JPC8-CRMRP W81XWH-16-1-0796 (Cullen) & MRMC W81XWH-15-1-0466 (Cullen)], the Department of Veterans Affairs [BLR&D Merit Review I01-BX003748 (Cullen)], the National Institutes of Health [BRAIN Initiative U01-NS094340 (Cullen) & NRSA Graduate Research Fellowship F31-NS090746 (Katiyar)], and the Center for Undergraduate Research and Fellowships at the University of Pennsylvania. Opinions, interpretations, conclusions and recommendations are those of the author(s) and are not necessarily endorsed by the Department of Defense, the Department of Veterans Affairs, or the National Institutes of Health.

bioRxiv preprint doi: https://doi.org/10.1101/847988; this version posted November 20, 2019. The copyright holder for this preprint (which was not certified by peer review) is the author/funder. All rights reserved. No reuse allowed without permission.

References

1 Grinsell, D. & Keating, C. P. Peripheral nerve reconstruction after injury: a review of clinical and experimental therapies. *Biomed Res Int* **2014**, 698256, doi:10.1155/2014/698256 (2014).

2 Lubinska, L. Patterns of Wallerian degeneration of myelinated fibres in short and long peripheral stumps and in isolated segments of rat phrenic nerve. Interpretation of the role of axoplasmic flow of the trophic factor. *Brain Res* **233**, 227-240 (1982).

3 Stoll, G., Griffin, J. W., Li, C. Y. & Trapp, B. D. Wallerian degeneration in the peripheral nervous system: participation of both Schwann cells and macrophages in myelin degradation. *J Neurocytol* **18**, 671-683 (1989).

4 Hall, S. Axonal regeneration through acellular muscle grafts. *J Anat* **190 (Pt 1)**, 57-71 (1997).

5 Fontana, X., Hristova, M., Da Costa, C., Patodia, S., Thei, L., Makwana, M., Spencer-Dene, B., Latouche, M., Mirsky, R., Jessen, K. R., Klein, R., Raivich, G. & Behrens, A. c-Jun in Schwann cells promotes axonal regeneration and motoneuron survival via paracrine signaling. *J Cell Biol* **198**, 127-141, doi:10.1083/jcb.201205025 (2012).

6 Webber, C. & Zochodne, D. The nerve regenerative microenvironment: early behavior and partnership of axons and Schwann cells. *Exp Neurol* **223**, 51-59, doi:10.1016/j.expneurol.2009.05.037 (2010).

7 Siemionow, M. & Brzezicki, G. Chapter 8: Current techniques and concepts in peripheral nerve repair. *Int Rev Neurobiol* **87**, 141-172, doi:10.1016/S0074-7742(09)87008-6 (2009).

8 Sakuma, M., Gorski, G., Sheu, S. H., Lee, S., Barrett, L. B., Singh, B., Omura, T., Latremoliere, A. & Woolf, C. J. Lack of motor recovery after prolonged denervation of the neuromuscular junction is not due to regenerative failure. *Eur J Neurosci* **43**, 451-462, doi:10.1111/ejn.13059 (2016).

9 Yu, K. & Kocsis, J. D. Schwann cell engraftment into injured peripheral nerve prevents changes in action potential properties. *J Neurophysiol* **94**, 1519-1527, doi:10.1152/jn.00107.2005 (2005).

10 Cavanagh, J. B. The significance of the "dying back" process in experimental and human neurological disease. *Int Rev Exp Pathol* **3**, 219-267 (1964).

11 Kaplan, H. M., Mishra, P. & Kohn, J. The overwhelming use of rat models in nerve regeneration research may compromise designs of nerve guidance conduits for humans. *Journal of materials science. Materials in medicine* **26**, 226, doi:10.1007/s10856-015-5558-4 (2015).

12 Gordon, T., Tyreman, N. & Raji, M. A. The basis for diminished functional recovery after delayed peripheral nerve repair. *J Neurosci* **31**, 5325-5334, doi:10.1523/JNEUROSCI.6156-10.2011 (2011).

13 Pfister, B. J., Gordon, T., Loverde, J. R., Kochar, A. S., Mackinnon, S. E. & Cullen, D. K. Biomedical engineering strategies for peripheral nerve repair: surgical applications, state of the art, and future challenges. *Critical reviews in biomedical engineering* **39**, 81-124 (2011).

14 Perlson, E., Maday, S., Fu, M. M., Moughamian, A. J. & Holzbaur, E. L. Retrograde axonal transport: pathways to cell death? *Trends Neurosci* **33**, 335-344, doi:10.1016/j.tins.2010.03.006 (2010).

15 Abe, N. & Cavalli, V. Nerve injury signaling. *Curr Opin Neurobiol* **18**, 276-283, doi:10.1016/j.conb.2008.06.005 (2008).

bioRxiv preprint doi: https://doi.org/10.1101/847988; this version posted November 20, 2019. The copyright holder for this preprint (which was not certified by peer review) is the author/funder. All rights reserved. No reuse allowed without permission.

16 Jivan, S., Novikova, L. N., Wiberg, M. & Novikov, L. N. The effects of delayed nerve repair on neuronal survival and axonal regeneration after seventh cervical spinal nerve axotomy in adult rats. *Exp Brain Res* **170**, 245-254, doi:10.1007/s00221-005-0207-7 (2006).

17 Campenot, R. B. Development of sympathetic neurons in compartmentalized cultures. II. Local control of neurite survival by nerve growth factor. *Dev Biol* **93**, 13-21 (1982).

18 Strom, A. L., Gal, J., Shi, P., Kasarskis, E. J., Hayward, L. J. & Zhu, H. Retrograde axonal transport and motor neuron disease. *J Neurochem* **106**, 495-505, doi:10.1111/j.1471-4159.2008.05393.x (2008).

19 Mendell, L. M. Neurotrophins and sensory neurons: role in development, maintenance and injury. A thematic summary. *Philos Trans R Soc Lond B Biol Sci* **351**, 463-467, doi:10.1098/rstb.1996.0043 (1996).

20 Terenghi, G. Peripheral nerve regeneration and neurotrophic factors. *J Anat* **194 (Pt 1)**, 1-14 (1999).

21 MacInnis, B. L. & Campenot, R. B. Retrograde support of neuronal survival without retrograde transport of nerve growth factor. *Science* **295**, 1536-1539, doi:10.1126/science.1064913 (2002).

22 Turner, J. E., Schwab, M. E. & Thoenen, H. Nerve growth factor stimulates neurite outgrowth from goldfish retinal explants: the influence of a prior lesion. *Brain Res* **256**, 59-66 (1982).

23 Oyelese, A. A., Rizzo, M. A., Waxman, S. G. & Kocsis, J. D. Differential effects of NGF and BDNF on axotomy-induced changes in GABA(A)-receptor-mediated conductance and sodium currents in cutaneous afferent neurons. *J Neurophysiol* **78**, 31-42, doi:10.1152/jn.1997.78.1.31 (1997).

24 Oudega, M. & Hagg, T. Nerve growth factor promotes regeneration of sensory axons into adult rat spinal cord. *Exp Neurol* **140**, 218-229, doi:10.1006/exnr.1996.0131 (1996).

25 Lin, G., Bella, A. J., Lue, T. F. & Lin, C. S. Brain-derived neurotrophic factor (BDNF) acts primarily via the JAK/STAT pathway to promote neurite growth in the major pelvic ganglion of the rat: part 2. *J Sex Med* **3**, 821-829, doi:10.1111/j.1743-6109.2006.00292.x (2006).

26 Pan, H. C., Cheng, F. C., Chen, C. J., Lai, S. Z., Lee, C. W., Yang, D. Y., Chang, M. H. & Ho, S. P. Post-injury regeneration in rat sciatic nerve facilitated by neurotrophic factors secreted by amniotic fluid mesenchymal stem cells. *J Clin Neurosci* **14**, 1089-1098, doi:10.1016/j.jocn.2006.08.008 (2007).

27 Frerichs, O., Fansa, H., Schicht, C., Wolf, G., Schneider, W. & Keilhoff, G. Reconstruction of peripheral nerves using acellular nerve grafts with implanted cultured Schwann cells. *Microsurgery* **22**, 311-315, doi:10.1002/micr.10056 (2002).

28 Pfister, L. A., Papaloizos, M., Merkle, H. P. & Gander, B. Nerve conduits and growth factor delivery in peripheral nerve repair. *J Peripher Nerv Syst* **12**, 65-82, doi:10.1111/j.1529-8027.2007.00125.x (2007).

29 Kim, B. S., Yoo, J. J. & Atala, A. Peripheral nerve regeneration using acellular nerve grafts. *J Biomed Mater Res A* **68**, 201-209, doi:10.1002/jbm.a.10045 (2004).

30 Struzyna, L. A., Harris, J. P., Katiyar, K. S., Chen, H. I. & Cullen, D. K. Restoring nervous system structure and function using tissue engineered living scaffolds. *Neural Regen Res* **10**, 679-685, doi:10.4103/1673-5374.156943 (2015).

31 Pfister, B. J., Gordon, T., Loverde, J. R., Kochar, A. S., Mackinnon, S. E. & Cullen, D. K. Biomedical engineering strategies for peripheral nerve repair: surgical applications, state of the art, and future challenges. *Crit Rev Biomed Eng* **39**, 81-124, doi:10.1615/critrevbiomedeng.v39.i2.20 (2011).

bioRxiv preprint doi: https://doi.org/10.1101/847988; this version posted November 20, 2019. The copyright holder for this preprint (which was not certified by peer review) is the author/funder. All rights reserved. No reuse allowed without permission.

32 Katiyar, K. S., Struzyna, L. A., Das, S. & Cullen, D. K. "Stretch-Growth" of Motor Axons in Custom Mechanobioreactors to Generate Long-Projecting Axonal Constructs. *J Tissue Eng Regen Med*, doi:10.1002/term.2955 (2019).

33 Huang, J. H., Cullen, D. K. c.-f. a., Browne, K. D., Groff, R., Zhang, J., Pfister, B. J., Zager, E. L. & Smith, D. H. Long-term survival and integration of transplanted engineered nervous tissue constructs promotes peripheral nerve regeneration. *Tissue Eng Part A* **15**, 1677-1685 (2009).

34 Pfister, B. J., Iwata, A., Meaney, D. F. & Smith, D. H. Extreme stretch growth of integrated axons. *J Neurosci* **24**, 7978-7983, doi:10.1523/JNEUROSCI.1974-04.2004 (2004).

35 Pfister, B. J., Iwata, A., Taylor, A. G., Wolf, J. A., Meaney, D. F. & Smith, D. H. Development of transplantable nervous tissue constructs comprised of stretch-grown axons. *J Neurosci Methods* **153**, 95-103, doi:10.1016/j.jneumeth.2005.10.012 (2006).

36 Huang, J. H., Cullen, D. K., Browne, K. D., Groff, R., Zhang, J., Pfister, B. J., Zager, E. L. & Smith, D. H. Long-term survival and integration of transplanted engineered nervous tissue constructs promotes peripheral nerve regeneration. *Tissue Eng Part A* **15**, 1677-1685, doi:10.1089/ten.tea.2008.0294 (2009).

37 Roberts, S. E., Thibaudeau, S., Burrell, J. C., Zager, E. L., Cullen, D. K. & Levin, L. S. To reverse or not to reverse? A systematic review of autograft polarity on functional outcomes following peripheral nerve repair surgery. *Microsurgery* **37**, 169-174, doi:10.1002/micr.30133 (2017).

38 Catapano, J., Willand, M. P., Zhang, J. J., Scholl, D., Gordon, T. & Borschel, G. H. Retrograde labeling of regenerating motor and sensory neurons using silicone caps. *J Neurosci Methods* **259**, 122-128, doi:10.1016/j.jneumeth.2015.11.020 (2016).

39 Abercrombie, M. Estimation of nuclear population from microtome sections. *Anat Rec* **94**, 239-247, doi:10.1002/ar.1090940210 (1946).

40 Katiyar, K. S., Struzyna, L. A., Morand, J. P., Burrell, J. C., Clements, B., Laimo, F. A., Browne, K. D., Kohn, J., Ali, Z., Ledebur, H. C., Smith, D. H. & Cullen, D. K. Tissue Engineered Axon Tracts Serve as Living Scaffolds to Accelerate Axonal Regeneration and Functional Recovery Following Peripheral Nerve Injury in Rats. *bioRxiv*, 654723 (2019).

41 Zhang, R. & Rosen, J. M. The role of undifferentiated adipose-derived stem cells in peripheral nerve repair. *Neural Regen Res* **13**, 757-763, doi:10.4103/1673-5374.232457 (2018).

42 Singh, D., Harding, A. J., Albadawi, E., Boissonade, F. M., Haycock, J. W. & Claeyssens, F. Additive Manufactured Biodegradable Poly(glycerol sebacate methacrylate) Nerve Guidance Conduits. *Acta Biomater*, doi:10.1016/j.actbio.2018.07.055 (2018).

43 Patel, N. P., Lyon, K. A. & Huang, J. H. An update-tissue engineered nerve grafts for the repair of peripheral nerve injuries. *Neural Regen Res* **13**, 764-774, doi:10.4103/1673-5374.232458 (2018).

44 Gonzalez-Perez, F., Hernandez, J., Heimann, C., Phillips, J. B., Udina, E. & Navarro, X. Schwann cells and mesenchymal stem cells in laminin- or fibronectin-aligned matrices and regeneration across a critical size defect of 15 mm in the rat sciatic nerve. *J Neurosurg Spine* **28**, 109-118, doi:10.3171/2017.5.SPINE161100 (2018).

45 Jiang, C. Q., Hu, J., Xiang, J. P., Zhu, J. K., Liu, X. L. & Luo, P. Tissue-engineered rhesus monkey nerve grafts for the repair of long ulnar nerve defects: similar outcomes to autologous nerve grafts. *Neural Regen Res* **11**, 1845-1850, doi:10.4103/1673-5374.194757 (2016).

46 Eren, F., Oksuz, S., Kucukodaci, Z., Kendirli, M. T., Cesur, C., Alarcin, E., Irem Bektas, E., Karagoz, H., Kerimoglu, O., Kose, G. T., Ulkur, E. & Gorantla, V. Targeted

bioRxiv preprint doi: https://doi.org/10.1101/847988; this version posted November 20, 2019. The copyright holder for this preprint (which was not certified by peer review) is the author/funder. All rights reserved. No reuse allowed without permission.

mesenchymal stem cell and vascular endothelial growth factor strategies for repair of nerve defects with nerve tissue implanted autogenous vein graft conduits. *Microsurgery* **36**, 578-585, doi:10.1002/micr.22401 (2016).

47 Tan, M., Yuan, M. Z., Sun, T. Y., Xie, Y. Y., Liu, L. L., Tang, Y., Ling, Z. M., Li, Y. Q., Yu, G. Y. & Zhou, L. H. Identification of the Avulsion-Injured Spinal Motoneurons. *J Mol Neurosci* **57**, 142-151, doi:10.1007/s12031-015-0588-4 (2015).

48 McPhail, L. T., McBride, C. B., McGraw, J., Steeves, J. D. & Tetzlaff, W. Axotomy abolishes NeuN expression in facial but not rubrospinal neurons. *Exp Neurol* **185**, 182-190 (2004).

49 Peyronnard, J. M., Charron, L., Lavoie, J. & Messier, J. P. Differences in horseradish peroxidase labeling of sensory, motor and sympathetic neurons following chronic axotomy of the rat sural nerve. *Brain Res* **364**, 137-150 (1986).

50 Moldovan, M., Sorensen, J. & Krarup, C. Comparison of the fastest regenerating motor and sensory myelinated axons in the same peripheral nerve. *Brain* **129**, 2471-2483, doi:10.1093/brain/awl184 (2006).

51 Cheah, M., Fawcett, J. W. & Haenzi, B. Differential regenerative ability of sensory and motor neurons. *Neurosci Lett* **652**, 35-40, doi:10.1016/j.neulet.2016.11.004 (2017).

52 Kunihiko Sasai, T. S., Haruhiko Watanabe, Shigeo Akagi, Ryokei Ogawa. Changes of regenerative capacity in proximal sites following peripheral nerve section in rabbit. *Journal of Orthopaedic Science* **2**, 342-348 (1997).

53 Rishal, I. & Fainzilber, M. Retrograde signaling in axonal regeneration. *Exp Neurol* **223**, 5-10, doi:10.1016/j.expneurol.2009.08.010 (2010).

54 Nehrt, A., Hamann, K., Ouyang, H. & Shi, R. Polyethylene glycol enhances axolemmal resealing following transection in cultured cells and in ex vivo spinal cord. *J Neurotrauma* **27**, 151-161, doi:10.1089/neu.2009.0993 (2010).

55 Howard, M. J., David, G. & Barrett, J. N. Resealing of transected myelinated mammalian axons in vivo: evidence for involvement of calpain. *Neuroscience* **93**, 807-815 (1999).

56 Pesaresi, M., Soon-Shiong, R., French, L., Kaplan, D. R., Miller, F. D. & Paus, T. Axon diameter and axonal transport: In vivo and in vitro effects of androgens. *Neuroimage* **115**, 191-201, doi:10.1016/j.neuroimage.2015.04.048 (2015).

57 Xia, C. H., Roberts, E. A., Her, L. S., Liu, X., Williams, D. S., Cleveland, D. W. & Goldstein, L. S. Abnormal neurofilament transport caused by targeted disruption of neuronal kinesin heavy chain KIF5A. *J Cell Biol* **161**, 55-66, doi:10.1083/jcb.200301026 (2003).

58 Firestone, A. J., Weinger, J. S., Maldonado, M., Barlan, K., Langston, L. D., O'Donnell, M., Gelfand, V. I., Kapoor, T. M. & Chen, J. K. Small-molecule inhibitors of the AAA+ ATPase motor cytoplasmic dynein. *Nature* **484**, 125-129, doi:10.1038/nature10936 (2012).

59 Melemedjian, O. K., Tillu, D. V. & Moy, J. K. Local translation and retrograde axonal transport of CREB regulates IL-6-induced nociceptive plasticity. *Molecular …* (2014).

60 Payne, S. C., Belleville, P. J. & Keast, J. R. Regeneration of sensory but not motor axons following visceral nerve injury. *Exp Neurol* **266**, 127-142, doi:10.1016/j.expneurol.2015.02.026 (2015).

61 Seijffers, R., Allchorne, A. J. & Woolf, C. J. The transcription factor ATF-3 promotes neurite outgrowth. *Mol Cell Neurosci* **32**, 143-154, doi:10.1016/j.mcn.2006.03.005 (2006).

62 Stenberg, L., Kanje, M., Dolezal, K. & Dahlin, L. B. Expression of activating transcription factor 3 (ATF 3) and caspase 3 in Schwann cells and axonal outgrowth after sciatic nerve repair in diabetic BB rats. *Neurosci Lett* **515**, 34-38, doi:10.1016/j.neulet.2012.03.011 (2012).

bioRxiv preprint doi: https://doi.org/10.1101/847988; this version posted November 20, 2019. The copyright holder for this preprint (which was not certified by peer review) is the author/funder. All rights reserved. No reuse allowed without permission.

63 Lindwall, C. & Kanje, M. Retrograde axonal transport of JNK signaling molecules influence injury induced nuclear changes in p-c-Jun and ATF3 in adult rat sensory neurons. *Mol Cell Neurosci* **29**, 269-282, doi:10.1016/j.mcn.2005.03.002 (2005).

64 Lloyd, B. M., Luginbuhl, R. D., Brenner, M. J., Rocque, B. G., Tung, T. H., Myckatyn, T. M., Hunter, D. A., Mackinnon, S. E. & Borschel, G. H. Use of motor nerve material in peripheral nerve repair with conduits. *Microsurgery* **27**, 138-145, doi:10.1002/micr.20318 (2007).

65 Nichols, C. M., Brenner, M. J., Fox, I. K., Tung, T. H., Hunter, D. A., Rickman, S. R. & Mackinnon, S. E. Effects of motor versus sensory nerve grafts on peripheral nerve regeneration. *Exp Neurol* **190**, 347-355, doi:10.1016/j.expneurol.2004.08.003 (2004).

66 Arslantunali, D., Dursun, T., Yucel, D., Hasirci, N. & Hasirci, V. Peripheral nerve conduits: technology update. *Med Devices (Auckl)* **7**, 405-424, doi:10.2147/MDER.S59124 (2014).

67 Kaplan, H. M., Mishra, P. & Kohn, J. The overwhelming use of rat models in nerve regeneration research may compromise designs of nerve guidance conduits for humans. *J Mater Sci Mater Med* **26**, 226, doi:10.1007/s10856-015-5558-4 (2015).

68 Moore, A. M., MacEwan, M., Santosa, K. B., Chenard, K. E., Ray, W. Z., Hunter, D. A., Mackinnon, S. E. & Johnson, P. J. Acellular nerve allografts in peripheral nerve regeneration: a comparative study. *Muscle Nerve* **44**, 221-234, doi:10.1002/mus.22033 (2011).

69 Isaacs, J. & Browne, T. Overcoming short gaps in peripheral nerve repair: conduits and human acellular nerve allograft. *Hand (N Y)* **9**, 131-137, doi:10.1007/s11552-014-9601-6 (2014).

70 Tang, P., Kilic, A., Konopka, G., Regalbuto, R., Akelina, Y. & Gardner, T. Histologic and functional outcomes of nerve defects treated with acellular allograft versus cabled autograft in a rat model. *Microsurgery* **33**, 460-467, doi:10.1002/micr.22102 (2013).

71 Georgiou, M., Bunting, S. C., Davies, H. A., Loughlin, A. J., Golding, J. P. & Phillips, J. B. Engineered neural tissue for peripheral nerve repair. *Biomaterials* **34**, 7335-7343, doi:10.1016/j.biomaterials.2013.06.025 (2013).

72 Wieringa, P. A., Goncalves de Pinho, A. R., Micera, S., van Wezel, R. J. A. & Moroni, L. Biomimetic Architectures for Peripheral Nerve Repair: A Review of Biofabrication Strategies. *Adv Healthc Mater* **7**, e1701164, doi:10.1002/adhm.201701164 (2018).

73 Daly, W., Yao, L., Zeugolis, D., Windebank, A. & Pandit, A. A biomaterials approach to peripheral nerve regeneration: bridging the peripheral nerve gap and enhancing functional recovery. *J R Soc Interface* **9**, 202-221, doi:10.1098/rsif.2011.0438 (2012).

74 Ruven, C., Badea, S. R., Wong, W. M. & Wu, W. Combination Treatment With Exogenous GDNF and Fetal Spinal Cord Cells Results in Better Motoneuron Survival and Functional Recovery After Avulsion Injury With Delayed Root Reimplantation. *J Neuropathol Exp Neurol* **77**, 325-343, doi:10.1093/jnen/nly009 (2018).

75 Nectow, A. R., Marra, K. G. & Kaplan, D. L. Biomaterials for the development of peripheral nerve guidance conduits. *Tissue Eng Part B Rev* **18**, 40-50, doi:10.1089/ten.TEB.2011.0240 (2012).

76 de Luca, A. C., Lacour, S. P., Raffoul, W. & di Summa, P. G. Extracellular matrix components in peripheral nerve repair: how to affect neural cellular response and nerve regeneration? *Neural Regen Res* **9**, 1943-1948, doi:10.4103/1673-5374.145366 (2014).

77 de Ruiter, G. C., Malessy, M. J., Yaszemski, M. J., Windebank, A. J. & Spinner, R. J. Designing ideal conduits for peripheral nerve repair. *Neurosurg Focus* **26**, E5, doi:10.3171/FOC.2009.26.2.E5 (2009).

78 Ramburrun, P., Kumar, P., Choonara, Y. E., Bijukumar, D., du Toit, L. C. & Pillay, V. A review of bioactive release from nerve conduits as a neurotherapeutic strategy for

bioRxiv preprint doi: https://doi.org/10.1101/847988; this version posted November 20, 2019. The copyright holder for this preprint (which was not certified by peer review) is the author/funder. All rights reserved. No reuse allowed without permission.

neuronal growth in peripheral nerve injury. *Biomed Res Int* **2014**, 132350, doi:10.1155/2014/132350 (2014).

79 Tajdaran, K., Gordon, T., Wood, M. D., Shoichet, M. S. & Borschel, G. H. A glial cell line-derived neurotrophic factor delivery system enhances nerve regeneration across acellular nerve allografts. *Acta Biomater* **29**, 62-70, doi:10.1016/j.actbio.2015.10.001 (2016).

80 Marquardt, L. M., Ee, X., Iyer, N., Hunter, D., Mackinnon, S. E., Wood, M. D. & Sakiyama-Elbert, S. E. Finely Tuned Temporal and Spatial Delivery of GDNF Promotes Enhanced Nerve Regeneration in a Long Nerve Defect Model. *Tissue Eng Part A* **21**, 2852-2864, doi:10.1089/ten.TEA.2015.0311 (2015).

81 Schmidt, C. E. & Leach, J. B. Neural tissue engineering: strategies for repair and regeneration. *Annu Rev Biomed Eng* **5**, 293-347, doi:10.1146/annurev.bioeng.5.011303.120731 (2003).

82 Santosa, K. B., Jesuraj, N. J., Viader, A., MacEwan, M., Newton, P., Hunter, D. A., Mackinnon, S. E. & Johnson, P. J. Nerve allografts supplemented with schwann cells overexpressing glial-cell-line-derived neurotrophic factor. *Muscle Nerve* **47**, 213-223, doi:10.1002/mus.23490 (2013).

83 Tannemaat, M. R., Eggers, R., Hendriks, W. T., de Ruiter, G. C., van Heerikhuize, J. J., Pool, C. W., Malessy, M. J., Boer, G. J. & Verhaagen, J. Differential effects of lentiviral vector-mediated overexpression of nerve growth factor and glial cell line-derived neurotrophic factor on regenerating sensory and motor axons in the transected peripheral nerve. *Eur J Neurosci* **28**, 1467-1479, doi:10.1111/j.1460-9568.2008.06452.x (2008).

84 Zhang, W., Fang, X., Zhang, C., Li, W., Wong, W. M., Xu, Y., Wu, W. & Lin, J. Transplantation of embryonic spinal cord neurons to the injured distal nerve promotes axonal regeneration after delayed nerve repair. *Eur J Neurosci* **45**, 750-762, doi:10.1111/ejn.13495 (2017).

85 Kurimoto, S., Kato, S., Nakano, T., Yamamoto, M., Takanobu, N. & Hirata, H. Transplantation of embryonic motor neurons into peripheral nerve combined with functional electrical stimulation restores functional muscle activity in the rat sciatic nerve transection model. *J Tissue Eng Regen Med* **10**, E477-E484, doi:10.1002/term.1844 (2016).

86 Mosahebi, A., Fuller, P., Wiberg, M. & Terenghi, G. Effect of allogeneic Schwann cell transplantation on peripheral nerve regeneration. *Exp Neurol* **173**, 213-223, doi:10.1006/exnr.2001.7846 (2002).

87 Gulati, A. K. Immune response and neurotrophic factor interactions in peripheral nerve transplants. *Acta Haematol* **99**, 171-174, doi:10.1159/000040832 (1998).

88 Smith, D. H., Burrell, J. C., Browne, K. D., Katiyar, K. S., Ezra, M. I., Dutton, J. L., Morand, J. P., Struzyna, L. A., Laimo, F. A., Chen, H. I., Wolf, J. A., Kaplan, H. M., Rosen, J. M., Ledebur, H. C., Zager, E. L., Ali, Z. & Cullen, D. K. Tissue Engineered Grafts Exploit Axon-Facilitated Axon Regeneration and Pathway Protection to Facilitate Functional Recovery Following 5 cm Peripheral Nerve Lesions in Swine. (Manuscript in Prep).

89 Chang, W., Shah, M. B., Lee, P. & Yu, X. Tissue-engineered spiral nerve guidance conduit for peripheral nerve regeneration. *Acta Biomater* **73**, 302-311, doi:10.1016/j.actbio.2018.04.046 (2018).